

The Editors encourage authors to publish research updates to this article type. Please follow the link in the citation below to view any related articles.



Citation: Kaur R, Meier CJ, McGraw EA, Hillyer JF, Bordenstein S. (2024) The mechanism of cytoplasmic incompatibility is conserved in Wolbachia-infected Aedes aegypti mosquitoes deployed for arbovirus control. PLoS Biol 22(3): e3002573. https://doi.org/10.1371/journal.pbio.3002573

Academic Editor: Mariana Federica Wolfner, Cornell University, UNITED STATES

Received: November 20, 2023
Accepted: March 1, 2024
Published: March 28, 2024

Copyright: © 2024 Kaur et al. This is an open access article distributed under the terms of the Creative Commons Attribution License, which permits unrestricted use, distribution, and reproduction in any medium, provided the original author and source are credited.

Data Availability Statement: All relevant data are within the paper and its Supporting information files.

Funding: This work was funded by National Institutes of Health Awards R01 Al132581 and Al143725 to S.R.B., National Institute of Allergy and Infectious Diseases R56 Al155573-01A1 to E. **UPDATE ARTICLE**

The mechanism of cytoplasmic incompatibility is conserved in *Wolbachia*-infected *Aedes aegypti* mosquitoes deployed for arbovirus control

Rupinder Kaur 1,2,3 *, Cole J. Meier 3 , Elizabeth A. McGraw 1,2,4 , Julian F. Hillyer 3 , Seth R. Bordenstein 1,2,3 *

- 1 Pennsylvania State University, Departments of Biology and Entomology, University Park, Pennsylvania, United States of America, 2 Pennsylvania State University, One Health Microbiome Center, Huck Institutes of the Life Sciences, University Park, Pennsylvania, United States of America, 3 Vanderbilt University, Department of Biological Sciences, Nashville, Tennessee, United States of America, 4 Pennsylvania State University, Center for Infectious Disease Dynamics, Huck Institutes of the Life Sciences, University Park, Pennsylvania, United States of America
- * r.kaur@psu.edu (RK); s.bordenstein@psu.edu (SRB)

Abstract

The rising interest and success in deploying inherited microorganisms and cytoplasmic incompatibility (CI) for vector control strategies necessitate an explanation of the CI mechanism. Wolbachia-induced CI manifests in the form of embryonic lethality when sperm from Wolbachia-bearing testes fertilize eggs from uninfected females. Embryos from infected females however survive to sustain the maternally inherited symbiont. Previously in Drosophila melanogaster flies, we demonstrated that CI modifies chromatin integrity in developing sperm to bestow the embryonic lethality. Here, we validate these findings using wMeltransinfected Aedes aegypti mosquitoes released to control vector-borne diseases. Once again, the prophage WO CI proteins, CifA and CifB, target male gametic nuclei to modify chromatin integrity via an aberrant histone-to-protamine transition. Cifs are not detected in the embryo, and thus elicit CI via the nucleoprotein modifications established pre-fertilization. The rescue protein CifA in oogenesis localizes to stem cell, nurse cell, and oocyte nuclei, as well as embryonic DNA during embryogenesis. Discovery of the nuclear targeting Cifs and altered histone-to-protamine transition in both Aedes aegypti mosquitoes and D. melanogaster flies affirm the Host Modification Model of CI is conserved across these host species. The study also newly uncovers the cell biology of Cif proteins in the ovaries, CifA localization in the embryos, and an impaired histone-to-protamine transition during spermiogenesis of any mosquito species. Overall, these sperm modification findings may enable future optimization of CI efficacy in vectors or pests that are refractory to Wolbachia transinfections.

A.M., and National Science Foundation Award 1949145 to J.F.H. The funders had no role in study design, data collection and analysis, decision to publish, or preparation of the manuscript.

Competing interests: S.R.B. and R.K. are listed as inventors on patents or provisional patents related to this work.

Abbreviations: AED, after egg deposition; CI, cytoplasmic incompatibility; CTCF, corrected total cell fluorescence; HM, Host Modification; PTM, posttranslational modification; SP, spermathecae; WMP, World Mosquito Program.

Introduction

Symbiotic biocontrol is a multifaceted strategy that uses microorganisms for positive health outcomes [1]. With the potential to save millions of lives when applied at a scale to global diseases, this approach is highly promising. One example is the recent, international success of deploying an intracellular bacterium of the alphaproteobacterial genus Wolbachia in mosquitoes to reduce the transmission of various RNA arboviruses to humans. Wolbachia express 2 key phenotypes in these control strategies. The first is a virus-blocking trait [2,3] that reduces the replication of RNA viruses such as dengue, Zika, and Chikungunya in the salivary glands of virus-transmitting mosquito females [4–9]. The second is a symbiotic drive system termed cytoplasmic incompatibility (CI) that results in embryonic lethality when Wolbachia-infected males mate with uninfected females [10]. The lethality results from catastrophic, paternal defects in early embryogenesis including failure in condensation and segregation of paternal chromosomes, chromatin bridging, shredding of the paternal nuclei, early embryonic arrest, regional mitotic failures, and nuclear fallout [11–18]. Females carrying the same strain of Wolbachia rescue this lethality, thereby conferring a strong fitness advantage that spreads Wolbachia in natural host populations [19–22]. The World Mosquito Program (WMP) and others leverage both the virus-blocking and CI traits of the wMel strain of Wolbachia from Drosophila melanogaster by stably transinfecting it into disease-transmitting Aedes aegypti mosquitoes that do not naturally carry Wolbachia [23,24]. Mass releases of these wMel-carrying mosquitoes lead to the conditional spread of Wolbachia via CI when the bacterial frequency exceeds an unstable equilibrium [25]. Indeed, upon successful releases, the WMP demonstrated 40% to 98% reductions in local dengue cases worldwide [26–33].

In transinfected *Ae. aegypti* mosquito hosts, *Wolbachia* induce strong CI [23,25,34], unlike in the natural host *D. melanogaster* where CI strength varies [35–43]. Variation in CI strength can depend on various factors such as *Wolbachia* levels in testes [44], host age [35–40], temperature [40–43], maternal symbiont densities [45], and relevant to this study, different *Wolbachia* genotypes interacting in their natural versus artificial host systems. For instance, in *D. simulans*, wRi induces nearly complete CI, while wNo and wHa strains induce lower levels of CI [46]. In the parasitoid wasp genus of *Nasonia*, wVitA of *N. vitripennis* causes incomplete CI in its native host but nearly complete CI in a related sibling host *N. giraulti* [47]. Whether different molecular mechanisms of CI operate by the same *Wolbachia* in varied hosts remains unknown and is the subject of this study.

The genetic basis of wMel cytoplasmic incompatibility is simple with 2 CI factor genes, cifA and cifB, encoded by WO prophage regions in the wMel genome. Dual transgenic expression in D. melanogaster testes causes CI, and cifA expression alone in ovaries rescues CI [14,48,49]. At the cellular level, Cif_{wMel} proteins act pre-fertilization to impair the histone-to-protamine transition during sperm development and establish CI [50]. Notably, neither of the Cif_{wMel} proteins were detected as paternally transferred to the fertilized Drosophila embryos. A similar study examined localization of wPip Cif proteins from Culex pipiens in the non-native host D. melanogaster. Using transgenic flies, a foreign $CifB_{wPip}$ variant in mature CI sperm transfers to the embryo upon fertilization and associates with paternal DNA replication stress [51]. However, paternal chromatin modifications established pre-fertilization in testes and in a wild-type host-Wolbachia system were not investigated [51].

Here, we asked the question whether or not *w*Mel transinfected into *Aedes aegypti* recapitulates the cell biological evidence in flies, namely for host modifications of nucleoprotein abundance in developing sperm and the lack of paternal CifB transfer to the embryo. This work thus tests if Cif proteins from the same strain of *Wolbachia* act mechanistically equivalent in native fly versus non-native mosquito hosts [52,53]. We used the WMP's *Ae. aegypti*

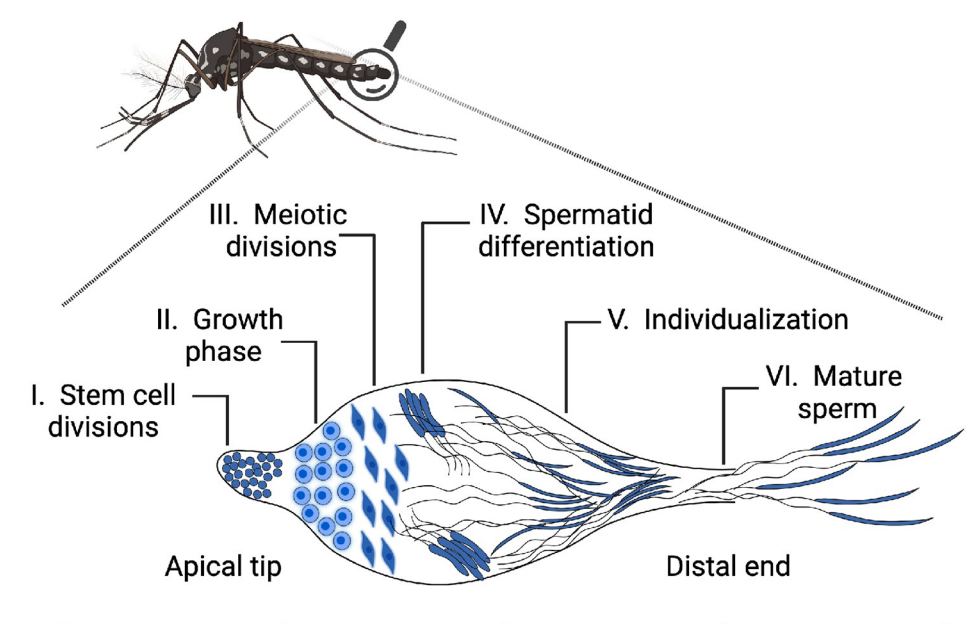
mosquitoes transinfected with wMel for the majority of the experiments and Ae. aegypti mosquitoes transinfected with the closely related variant wMelM [24]. Both strains induce strong CI with 100% identity in the cifA and cifB gene sequences. We report that results mostly recapitulated our previous findings in the native, wMel-infected D. melanogaster host [50]. During mosquito spermiogenesis, wMel Cifs impact paternal chromatin organization by modifying the abundance of histone and protamine nucleoproteins. Paternal transfer of Cif proteins to the fertilized mosquito embryos was not observed, indicating the sperm modified before fertilization establish the paternal-effect lethality of embryos. We further report that CifA occurs in oocytes and embryos of wMel-infected female mosquitoes that rescue CI, which is a new observation since CifA was not detectable in D. melanogaster embryos. We examine these different findings in the discussion. Overall, the CI/rescue drive system at the heart of vector control efforts depends on nuclear targeting Cif proteins in testes and ovaries. Ensuing modification of developing sperm leads to a disrupted histone-to-protamine transition and thus altered sperm chromatin integrity.

Results

wMel CifA and CifB proteins in Ae. aegypti target nuclei of developing sperm

To examine the cellular localization of wMel Cif proteins during sperm development, we used our developed Cif $_{w}$ Mel antibodies in Ae. aegypti males [50]. Testes organization in Ae. aegypti resembles a follicle with different compartments termed cysts (Fig 1) [54,55]. From the apical end to the base of a testis, cysts progressively increase in size and maturity so that smaller compartments with undifferentiated spermatogonia are found on the apical end, whereas larger cysts containing mature sperm are located at the base or the distal end. As maturation proceeds in the testes, spermatogonia grow, proliferate, and differentiate into spermatocytes. Spermatocytes then enter meiosis to generate haploid spermatids, which finally develop into spermatozoa via cytodifferentiation in a process known as spermiogenesis. The dramatic remodeling of the initially leaf-shaped spermatids includes nuclear condensation and elongation forming a sperm head and tail opposite to it. Finally, after individualization, the needle-shaped spermatids develop into mature sperm and release into the seminal vesicle [54,55].

We found that CifA localized in the nuclei of germline stem cells at the apical end of testes, whereas CifB occurred in the surrounding cytoplasm in 4 to 5 days old virgin mosquito males (Fig 1). In spermatocytes, both CifA and CifB were cytoplasmic and then acutely transported to the nuclei of postmeiotic leaf stage spermatids, depicting a cytonuclear transfer during the sperm morphogenesis process. Upon elongation, CifA localized to the cytoplasmic periphery of elongating spermatids, suggesting shuttling of the protein back to the cytoplasm, whereas CifB remained nuclear. After nuclear compaction, CifA stripped down along the tails of needle-shaped spermatids, and CifB remained colocalized with the spermatid head. Mature sperm extracted from the distal end of the testes demonstrated CifA remained with the sperm tail and CifB occurred with both the head and tail of sperm. CifA's presence in all sperm heads was observed in 2/10 testes examined in one experimental run (S1A Fig). Since Wolbachia were not present in the mature sperm, these results specify that Cif proteins are secreted out of bacterial cells to invade and interact with nuclei and cytoplasm of developing sperm cells. In Wolbachia-uninfected (wMel-) control testes, no CifA and CifB signals were detected, as expected (S1B Fig).



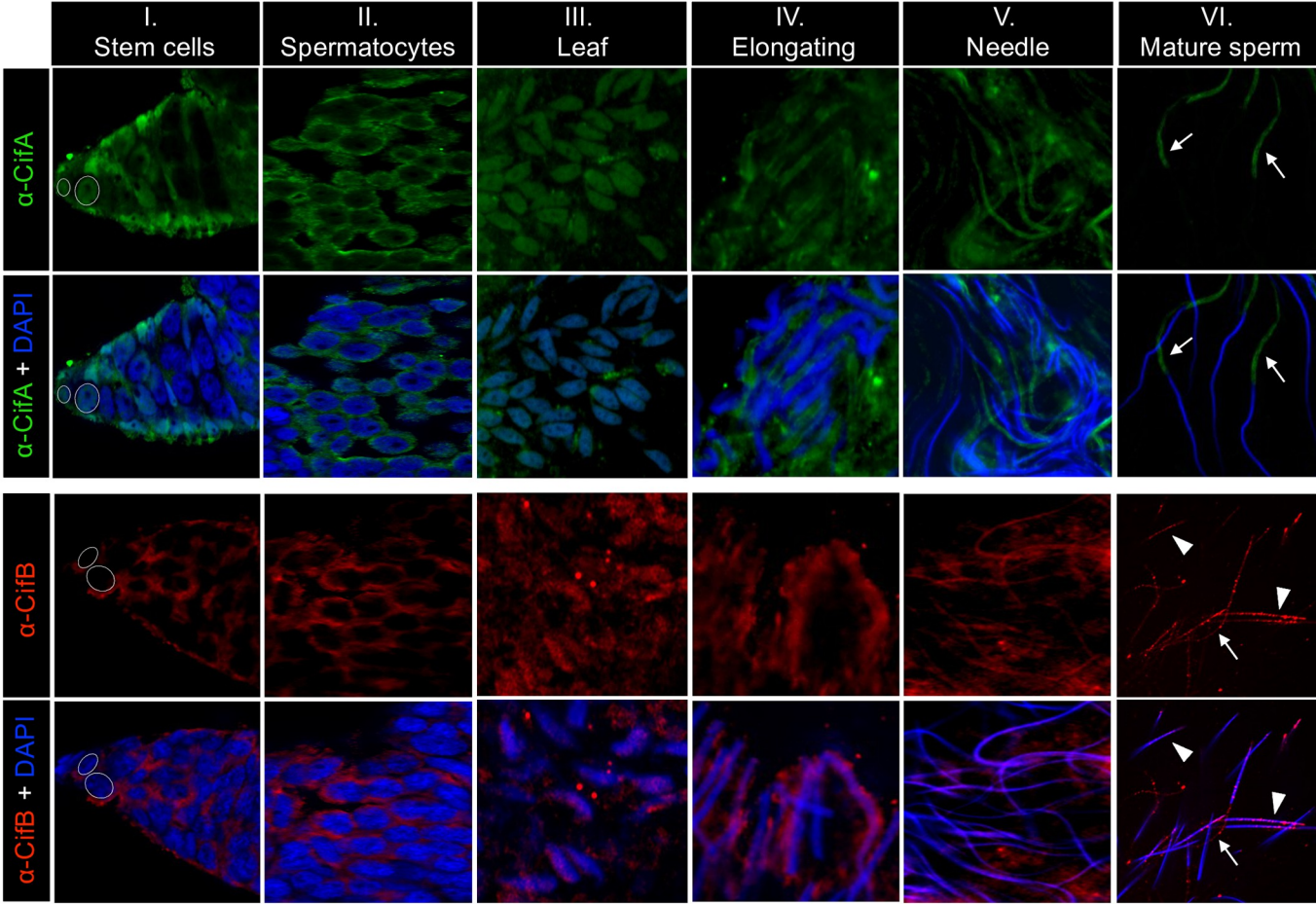


Fig 1. CifA and CifB exhibit cytoplasmic and nuclear localizations during sperm development in *Aedes aegypti*. Schematic representation of *Ae. aegypti* male mosquito and magnified reproductive system created with Biorender.com is shown on the top. From the apical end to the base of a testis, cysts progressively increase in size and maturity so that smaller compartments with undifferentiated spermatogonia are found on the apical end, whereas larger cysts containing mature sperm are located at the base or the distal end. *Wolbachia*-infected (*w*Mel+) testes (*n* = 10) from 4 to 5 days old virgin males were dissected and immunostained to visualize CI proteins, CifA (green) and CifB (red), during sperm morphogenesis. DAPI stain (blue) was used to label host nuclei. (I) At the

apical end of testes, CifA localizes to germline stem cell nuclei (white circles) with faint signals in the cytoplasm, whereas CifB is strictly in the cytoplasm. (II) Both CifA and CifB localize in the cytoplasm of mitotic spermatocytes in the growth phase and (III) migrate to the nuclei of postmeiotic leaf-stage spermatids, indicating CifA's cytonuclear exchange behavior. (IV–V) In the later differentiating stages of spermiogenesis, the elongating spermatids harbor CifA surrounding the nuclear periphery, which then strips down along the sperm tail during the tightly compacted, individualized, needle-stage spermatid formation. CifB, on the other hand, decorates the nuclear heads during elongation and penetrates the condensed needle stage nuclei. (VI) Upon full maturation, CifA is at the sperm tail (arrows), and CifB localizes in the form of dense punctae in both mature sperm head (arrowheads) and tail (arrows). Occasionally, CifA's presence in mature sperm head and not the tail was also detected in 2 out of 10 testes examined, with a similar puncta-based localization pattern of CifB (S1A Fig). CifA and CifB signals are absent in Wolbachia-uninfected (wMel–) negative control mosquitoes (S1B Fig). The experiment was repeated twice independently.

https://doi.org/10.1371/journal.pbio.3002573.g001

wMel hijacks the evolutionary-conserved, histone-to-protamine transition of developing sperm

Proper sperm chromatin integrity is crucial for successful fertilization and embryogenesis. During spermiogenesis, histone-bound chromatin is changed to a protamine-bound one that tightly condenses sperm DNA to package the sperm head [56]. However, mispackaged sperm due to an abnormal histone-to-protamine transition can cause male infertility and embryonic lethality in diverse systems from insects to mice [57,58]. Thus, to characterize Cifs' impact on the developing sperm chromatin organization of Ae. aegypti, we first investigated histone dynamics in infected (wMel+) and uninfected (wMel-) testes using an antibody targeting core histones conserved by sequence and structure across eukaryotes [59,60]. We found 2.01-fold significantly higher core histone intensity in wMel+ elongating spermatids (median = 3,764) compared to wMel- (median = 1,867) (Fig 2A and 2B and S1 Table). The increased histone retention persisted in the form of puncta on the wMel+ needle spermatid (Figs 2A and S2). Upon isolating mature sperm out of the testes, we consistently found a marked and significant increase in the percentage of wMel+ sperm (median = 92.5%) with retained histone puncta compared to wMel- (median = 0%) (Fig 2A and 2C and S1 Table). To detect whether the abnormal histone retention in mature sperm is associated with compounding errors in the histone-to-protamine transition, we used the fluorochrome chromomycin A3 (CMA3) stain that fluoresces upon binding to protamine-deficient regions of DNA [61]. Mature sperm isolated from wMel+ exhibited a similar 2.1-fold significant increase in CMA3 intensity consistent with protamine deficiency (median = 361.1) relative to wMel- (median = 169.7) (Fig 2D and 2E and S1 Table). Notably, this is the first characterization of an impaired histone-to-protamine transition through spermiogenesis in a mosquito species.

Protamine-deficient sperm travel with Cifs to the female reproductive tract

To investigate if sperm chromatin modifications and Cif proteins transfer paternally to females after mating, we crossed freshly hatched virgin wMel+ or wMel- males with virgin wMel-females in single pair mating. Individuals mated for 4 days to ensure mating. On day 5, the reproductive tract of females together with the spermathecae (SP)—a set of 3 rigid capsules that store, protect, and nourish sperm [62]—were dissected, and SPs were squashed to disentangle the sperm mass (Fig 3A). CI-sperm derived from wMel+ males transferred to SP of mated wMel- females showed a 1.37-fold significant increase in protamine deficiency (median = 2,717.43) compared to sperm derived from wMel- males (median = 1,974.29) (Fig 3B and 3C and S1 Table). Following Cif antibody staining, we detected CifA on the sperm tail and CifB on the sperm head and tail (Fig 3D), similar to their localization pattern in sperm isolated from testes (Fig 1). Using the histone antibody, we detected no histone signals on sperm isolated from females mated with both wMel+ and wMel- males (Fig 3D), suggesting that histone retention is temporary because they may be lost or degraded before mating or during transfer to the female SP.

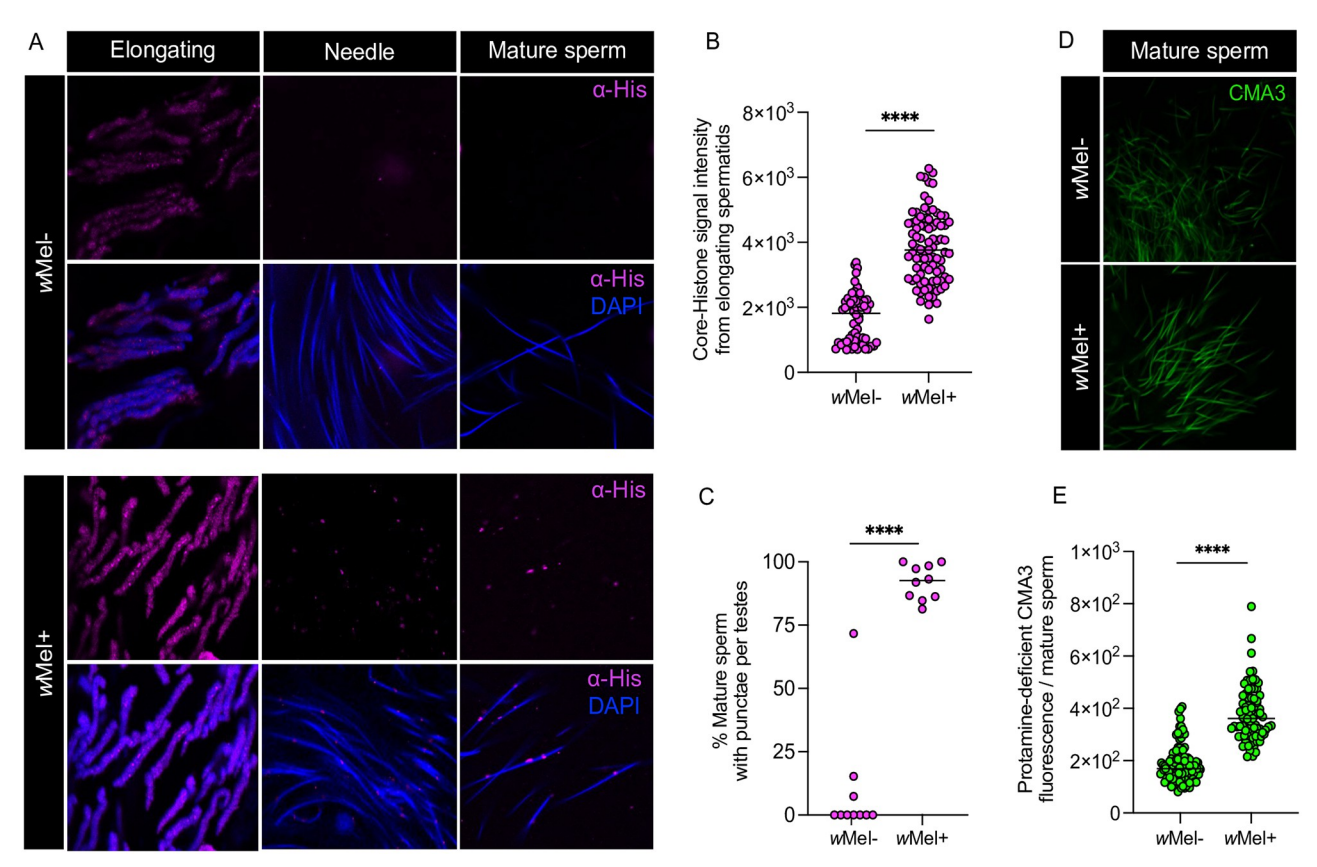


Fig 2. Maturing CI sperm abnormally retain histones and lack protamines. (A) wMel+ and wMel- testes (n = 10) from 4 to 5 days old virgin males were dissected and immunostained to visualize and quantify histone abundance (magenta) in elongating spermatids and mature sperm during sperm morphogenesis in Ae. aegypti. DAPI stain (blue) was used to label spermatid nuclei. (A, B) During the elongating stage, wMel+ males show higher core histones signal intensity than in wMel- males. (A, C) In the late maturation stages, wMel+ males show prolonged histone retention in the form of puncta in condensing needle-stage spermatids and individual mature sperm, whereas histones are removed in wMel- males as expected. A full uncropped image of needle spermatids with retained histones in wMel+ versus wMel- testes is shown in S2 Fig. (D) Fully mature sperm were extracted from wMel+ and wMel- testes (n = 10) of 4 to 5 days old virgin males and stained with fluorescent CMA3 (green) for detection of protamine deficiency. Signal intensity in each individual sperm nucleus head was quantified in ImageJ (see Methods) and graphed. wMel+ sperm show enhanced protamine deficiency levels compared to wMel- control. Horizontal bars in (B), (C), and (E) represent median value. Statistical significance (p < 0.05) was determined by running pairwise comparisons based on Kolmogorov—Smirnov test. All the p-values are reported in S1 Table. The experiments were performed in two independent biological replicates. Raw data underlying this figure can be found in S1 Data file.

Paternal CifA and CifB are not detected in CI embryos; maternal CifA is present in rescue embryos

Once fertilization occurs, the canonical cellular consequences of CI are delayed paternal chromatin condensation, paternal chromatin bridges, and segregation defects resulting in early, and in some cases, mid-stage embryonic arrest [12–14,17,18,63–67]. In *Ae. aegypti*, the male pronucleus is formed within 1 h after fertilization, followed by apposition and 2 successive mitotic divisions producing 4 nuclei between 1 and 2 h [68]. By 3 h, asynchrony of nuclear divisions occurs where mitotic nuclei in various stages of divisions are widely scattered over the deutoplasm, the yolk reserve of the egg.

To investigate if paternal Cif proteins loaded in the sperm head and tail transfer to the embryos after fertilization, we performed 3 crosses: wMel+ males $\times w$ Mel- females (CI cross), wMel+ males $\times w$ Mel+ females (Rescue cross), and wMel- males $\times w$ Mel- females (negative

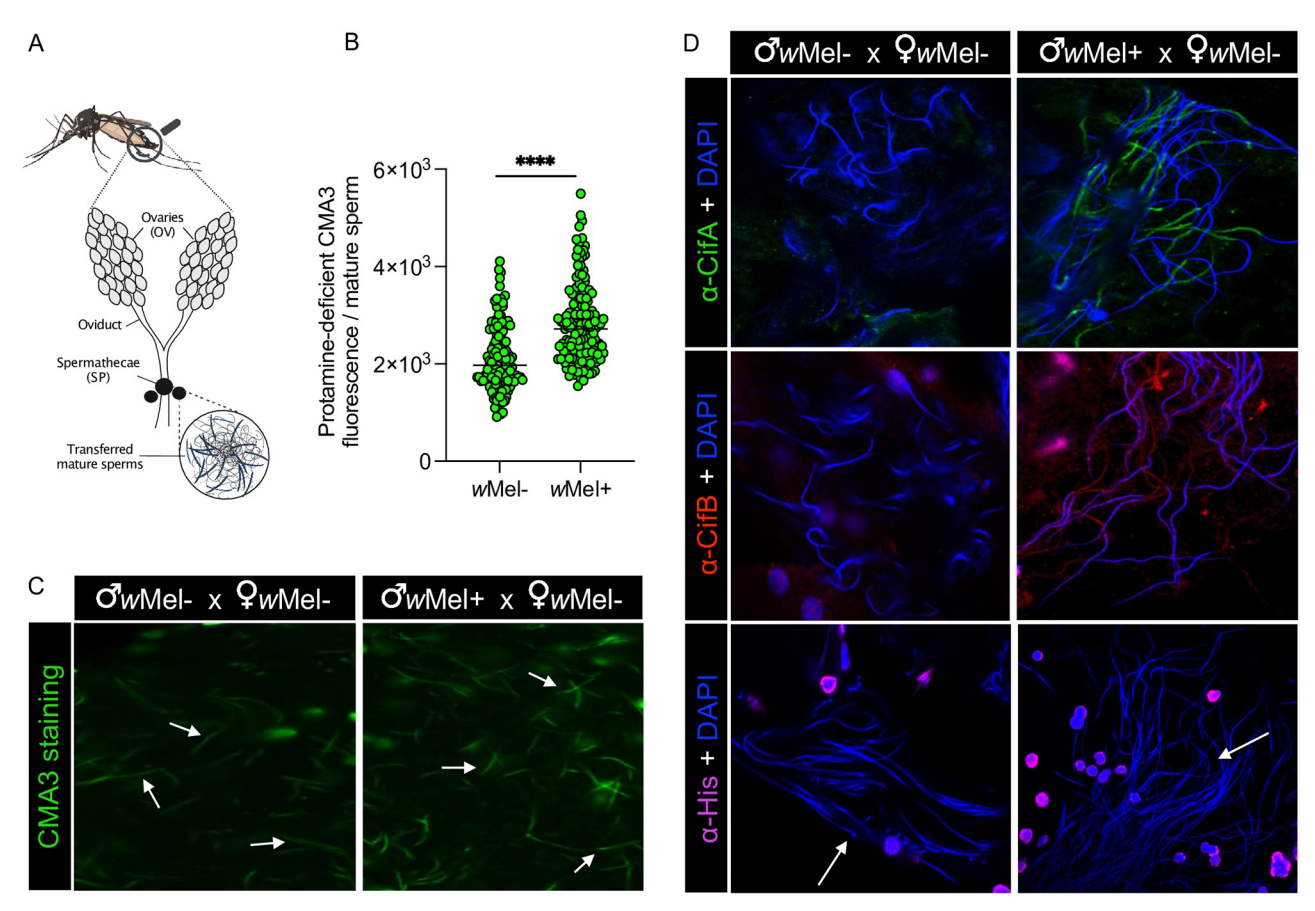


Fig 3. Protamine deficiency and Cifs persist in mature sperm transferred to spermathecae of uninfected females, whereas histones do not. (A) Schematic representation of $Ae.\ aegypti$ female reproductive system, created with BioRender.com that shows ovaries (OV) and spermatheca (SP), the specialized sperm storage organ. wMel+ and wMel- males were mated in single pair to wMel- females. Females were then dissected, and transferred sperm were released by puncturing SP. (B) Individual sperm head intensity quantification shows that sperm protamine deficiency from wMel+ males persist after transfer in the females compared to that of wMel- males. Horizontal bars represent median value. Statistical significance (p < 0.05) was determined by running pairwise comparisons based on a Kolmogorov—Smirnov test. The p-values are reported in S1 Table, and raw data underlying panel B of this figure can be found in S1 Data file. (C) Representative images of CMA3-stained mature sperm (arrows) transferred from wMel- and wMel+ males in wMel- female reproductive systems are shown. (D) Isolated sperm from females were immunostained for localizing CifA (green), CifB (red), and histones (magenta). DAPI stain (blue) was used to label nuclei. In sperm derived from wMel+ males, CifA is predominantly seen along the sperm tail and CifB on both sperm head and tail. Both CifA and CifB signals are absent in sperm from wMel- males. Histone puncta earlier detected in mature sperm from wMel+ testes are not present in sperm extracted from female tract (arrows). All the experiments were performed in 2 independent biological replicates.

control). We collected embryos in 0 to 3 h intervals after egg deposition (AED) followed by immunostaining. In approximately 1.5 h old CI embryos, the expected chromatin catastrophes occurred, including fragmented DNA (Fig 4A) and under-condensed nuclear DNA partially scattered in the egg yolk cytoplasm (Fig 4A'). Importantly, neither CifA nor CifB was detected in CI embryos, whereas control histone signals were observed colocalizing with nuclear DNA. These results indicate that Cifs are likely not paternally delivered via sperm to the mosquito embryo, similar to our previous findings in flies [50].

In approximately 1 h old rescue embryos, we observed synkaryon that forms after maternal and paternal pronucleus appose each other. Maternally derived CifA partially overlapped with DNA and predominantly concentrated around the periphery of a putative group of chromosomes at metaphase (Fig 4B). The end of the third nuclear cycle in approximately 2 h old

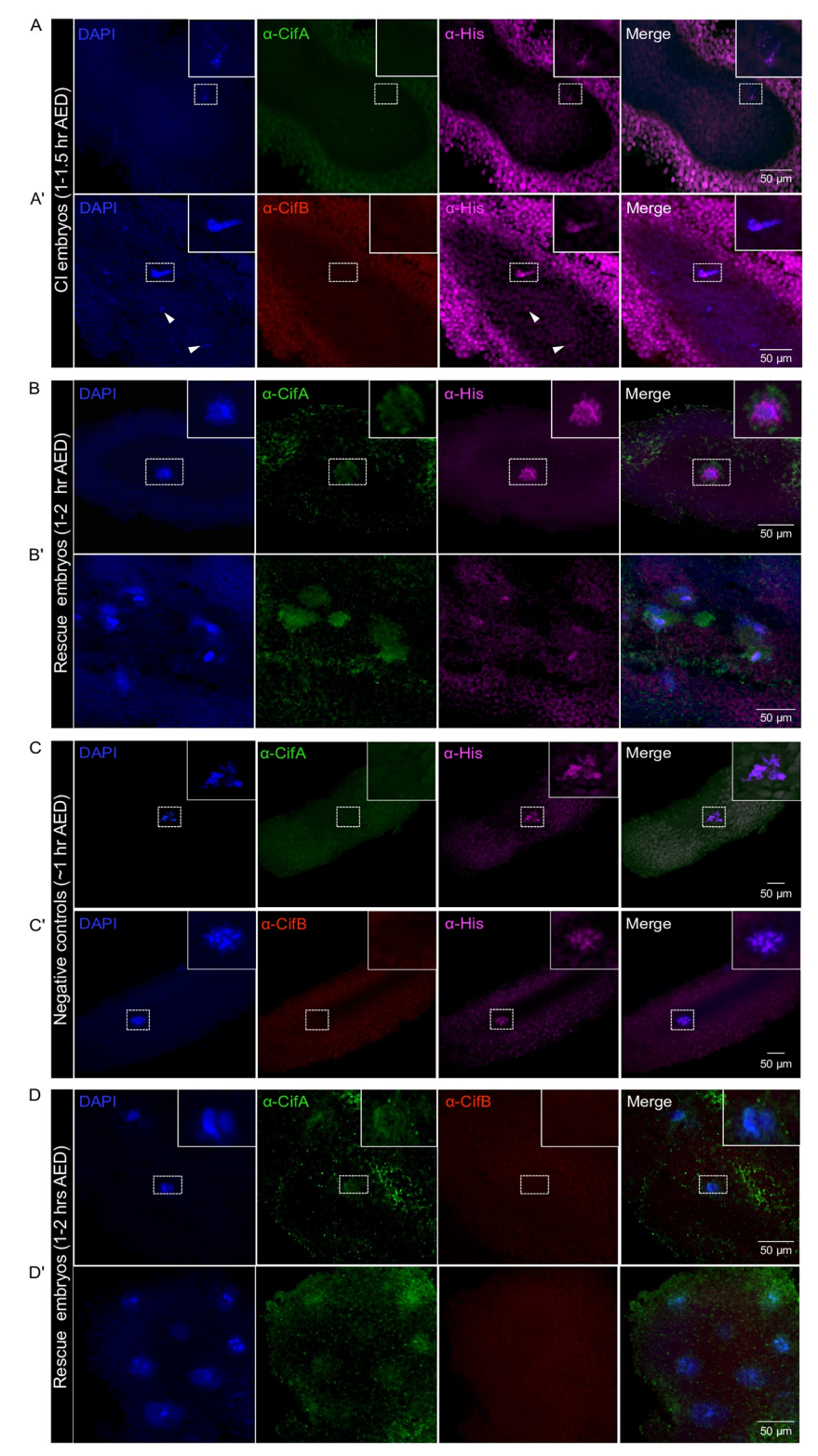


Fig 4. CifA and CifB are not paternally delivered to the *Ae. aegypti* CI embryos; CifA is detected in the rescue embryos. Immunofluorescence of CifA (green) and CifB (red) was performed in 1–3 h old, fertilized *Ae. aegypti* embryos (*n* = 15) each obtained from CI cross (*w*Mel+ male × *w*Mel− female), rescue cross (*w*Mel+ male × *w*Mel + female), and negative control cross (*w*Mel- male × *w*Mel- female). Host DNA was labeled with DAPI (blue), and core histone (magenta) was used as a positive antibody control. In 1–1.5 h AED old CI embryos, (A) nuclei fragmentation

and (A') shredding characteristics were observed (arrowheads). Histone signals were detected colocalizing with host DNA, whereas no CifA and CifB signals delivered from paternal sperm were detected. Dotted box is drawn around the chromosomal DNA with magnified view shown in the inset at the upper right corner. (B) In approximately 1 h AED old rescue embryos, CifA localizes in and around the periphery of chromosomal DNA putatively separating at metaphase. (B') At approximately 2 h AED during nuclear cycle 3, CifA localizes with nuclear DNA and surrounding cytoplasm of 8 daughter cells in rescue embryos (\$3 Fig). (C, C') Approximately 1 h old negative control embryos showed positive histone signals colocalizing with chromosomal DNA and absence of both CifA and CifB, as expected. (D, D') Further, to investigate whether CifA and CifB could bind in the fertilized rescue embryo, we used both antibodies together (see Methods) and once again validated no transfer of paternal CifB and consistent nuclear and peripheral signals of maternal CifA. We note the autofluorescence due to yolk fat cells and green dots are background noise likely due to the presence of unwashed residual antibody.

https://doi.org/10.1371/journal.pbio.3002573.g004

rescue embryo resulted in 8 daughter nuclei, where CifA is detected in and around each daughter cell nucleus (Figs 4B' and S3). In the negative control approximately 1 h old embryos, histone signals colocalized with segregating chromosomal DNA, and no CifA and CifB signals were detected, as expected (Fig 4C and 4C'). We also tested whether CifA and CifB may bind together in early 1 to 2 h old, fertilized, rescue embryos by co-staining with both Cif antibodies (see Methods). While consistent signals of CifA co-localized with DNA, there was no evidence of CifB presence in embryos during initial and subsequent mitotic divisions (Fig 4D and 4D'). In late rescue embryos collected at approximately 3 h AED, we consistently detected concentrated patchy signals of CifA adjoining the periphery of separating chromosomes at anaphase and in the cytoplasm of divided nuclei at 4 to 5 and later division cycles, respectively (Fig 5A and 5A'). In contrast, the CI embryos collected at the same time showed disrupted nuclear divisions and no signals of neither CifA nor CifB (Fig 5B and 5B'), indicating a lack of evidence for paternal Cif transfer to the fertilized embryos.

If Cif expression in these early embryos is regulated by maternally inherited *Wolbachia* cells, then we expect gene expression levels to be high for CifA and low for CifB. qPCR analysis of *cif* gene expression in embryos carrying *w*MelM collected 0 to 2 h AED indeed confirm this expectation with an order of magnitude higher expression for *cifA* (S4 Fig). It remains possible that the CifB protein is not translated due to the low mRNA levels detected. An alternative explanation for the presence of CifA and absence of CifB in early rescue embryos is that CifA is inherited with maternal DNA from the oocyte to the embryo (see below section).

CifA localizes to the nuclei of germline stem cells, nurse cells, and oocyte during oogenesis in females

The transgenic basis of rescue is specifically dependent on wMel CifA expression in fly and mosquito ovaries [48,49,69]. The *in situ* localization dynamics of CifA in mosquito ovaries has not been evaluated to date. Unlike *Drosophila*, oogenesis in *Ae. aegypti* occurs in 2 stages (Fig 6A and 6B). The first pre-vitellogenic stage occurs before females feed on blood and specifically affiliates with an increase in primary ovarioles [70]. The second vitellogenic stage starts after blood feeding and associates with deposition of yolk proteins and lipids from the fat body, and RNA and proteins from nurse cells into developing oocytes [71,72]. Oocyte maturation then leads to egg deposition [55,73]. In *Ae. aegypti* ovaries, nutritional provisioning via the blood meal is crucial since eggs cannot exogenously source nutrients, and all nutritional requirements for embryogenesis must be packaged during oogenesis [74].

We tracked wMel Wolbachia and CifA localization in ovaries before and after blood feeding. In both blood fed and non-blood fed females, Wolbachia resided in the cytoplasm of germline stem cells, nurse cells, and the oocyte, as expected (Figs 6 and S5). In contrast, CifA localization was mainly nuclear. Before blood feeding, CifA occurred in stem cell nuclei in the

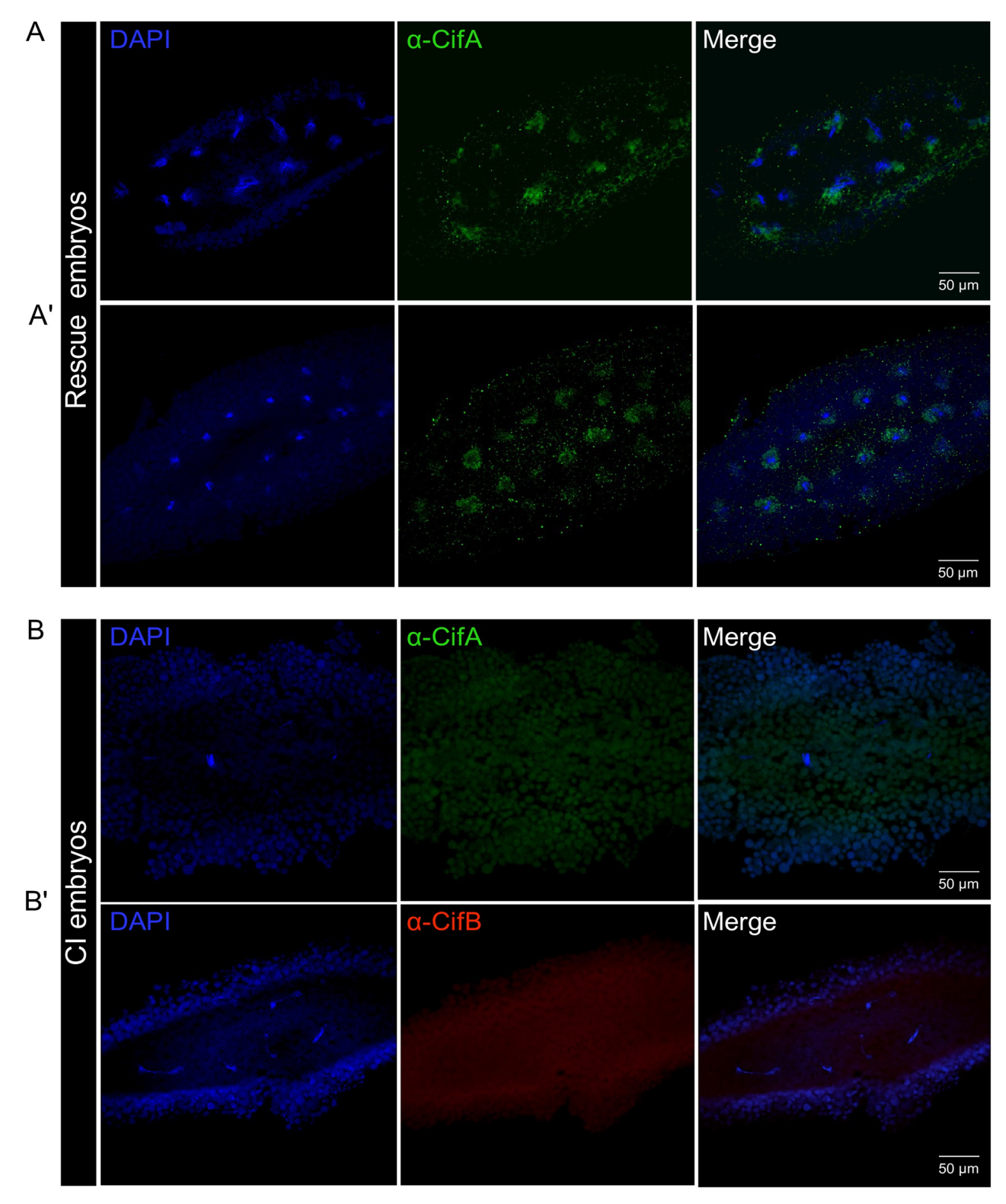


Fig 5. CifA remains attached to the chromosomes and in cytoplasmic periphery around the nuclei in late-stage rescue embryos, whereas CifB is undetected. Late-stage CI and rescue embryos collected at approximately 3 h AED were immunostained with CifA and CifB antibodies. We consistently detected concentrated patchy signals of CifA adjoining the periphery of separating chromosomes at anaphase and in the cytoplasm of divided nuclei at 4 to 5 and later division cycles, respectively (Fig 5A and 5A'). In contrast, the CI embryos collected at the same time showed disrupted nuclear divisions and no signals of neither CifA nor CifB (Fig 5B and 5B').

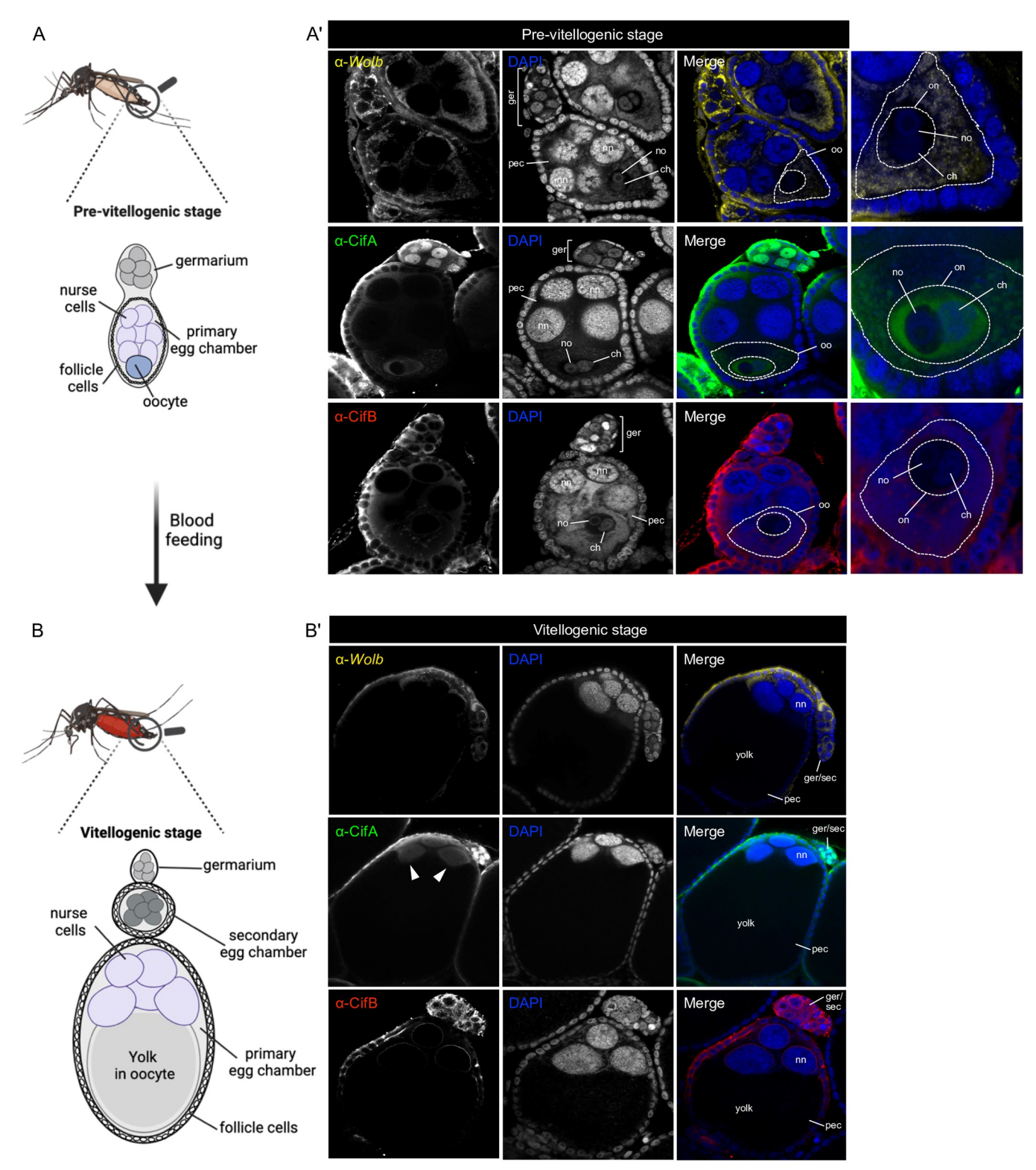


Fig 6. Compared to cytoplasmic *Wolbachia* and CifB in the *Ae. aegypti* ovaries, CifA exhibits nuclear localization in germarium, nurse cells and oocyte nuclei. (A, B) Schematic representation of *Ae. aegypti* ovary on the left illustrates the stages of oogenesis pre- and post-blood feeding, created with Biorender. com. Ovaries (n = 10) from 4 to 5 days old females were dissected before and 24 h after blood feeding. (A') Immunostaining assay shows that in non-blood fed *w*Mel+ females, *Wolbachia* (yellow) and CifB (in red) localize in the cytoplasm of germarium (ger), nurse cells, and oocyte (oo). CifA (green), on the other hand, is present in the nuclei of germ cells and the peripheral cytoplasm of nurse cells in the primary egg chamber (pec). Occasionally, CifA occurs in nurse cell nuclei

(nn) (S4 Fig). In the oocyte, CifA is nuclear (on) inhabiting nucleoplasm space containing chromatin mass (ch) and a nucleolus (no). CifA colocalizes with chromatin outside of the nucleolus area. (B) After blood feeding, *Wolbachia* and CifB in *w*Mel+ females remain cytoplasmic in germarium and at the periphery of nurse cells. CifA remains nuclear in germline stem cells, secondary egg chamber (sec), and nurse cells (arrowheads) in pec. After blood intake, oocyte size grows dramatically filled with yolk (black zone) in the pec. *w*Mel- females before and after blood feeding are devoid of any *Wolbachia* and CifA and CifB signals, as expected (S5 Fig). In the ovaries of both *w*Mel+ and *w*Mel- lines, we note that the occasionally observed autofluorescence in red, green, and yellow channels outlining the tissue morphology does not signify *Wolbachia*, CifA, and CifB signals, respectively.

https://doi.org/10.1371/journal.pbio.3002573.g006

germarium (GSCs) and in the cytoplasm near follicle cells and nurse cells in the primary egg chamber (Fig 6A'). Occasionally, CifA was detected colocalizing with nurse cell nuclei (n = 3/10 ovaries examined) (S6 Fig). The *Ae. aegypti* mosquito oocyte comprises an uncommon nucleus with 2 distinct bodies—nucleolus and chromosomal mass [75,76]. In the oocyte nucleus, CifA inhabits the nucleoplasm containing the chromatin mass and does not enter in the nucleolus (Figs 6A' and S6). CifA's presence in the oocyte nucleus together with the nuclear chromosomal mass suggests its potential interaction with maternal chromatin early in oogenesis, possibly to prime the rescue process. We also tracked CifB localization that, like *Wolbachia*, was found strictly cytoplasmic around germline stem cells, nurse cells, and oocyte nuclei (Fig 6A').

After blood feeding and as vitellogenesis proceeds, the primary egg chamber increases in size due to an oocyte packed with non-staining yolk particles. CifA persisted in the GSCs and nurse cell nuclei, whereas CifB remained cytoplasmic surrounding the periphery of nurse cell nuclei in primary egg chamber (Fig 6B'). In the large oocyte, we did not detect either of the proteins likely because the antibody did not penetrate through the vitelline membrane in a whole-mount insect tissue preparation [77–79]. Overall, results indicate that CifA targets the nuclei of ovarian germline, nurse cells, and oocyte in a manner that could facilitate host nuclear modification for rescue either earlier in oogenesis or embryogenesis. The finding also corroborated the discovery of CifA's nuclear localization signal, which is not present in CifB [50].

Discussion

Large-scale deployments of Wolbachia-infected Ae. aegypti mosquitoes result in population replacement of Wolbachia-uninfected mosquitoes with wMel symbiotic individuals, and concordantly, a 40% to 98% reduction in local dengue cases. This relatively new strategy for arboviral disease control is an excellent example of deploying microbial symbionts for positive health outcomes, and it is likely extendable to agriculture health by reducing the burden of crop infectious diseases as well [80]. The main goal of our study was to decipher the cellular and molecular mechanisms of the wMel CI drive system responsible in major part for the population replacement success stories of the WMP. We report below previously unknown aspects of mosquito reproductive biology in relation to symbiotic control: (i) The CI-causing Cif proteins from wMel Wolbachia invade nuclei of developing sperm of Ae. aegypti mosquitoes and cause an abnormal histone-to-protamine transition, a conserved and essential step for normal sperm metamorphosis and genome packaging [56,81]. (ii) Histone—protamine dynamics were obscure in the mosquito literature, and this work provides the first characterization of this transition under the influence of wMel Wolbachia in a mosquito host species relevant for human health. (iii) Mature sperm with protamine deficiency are transferred to the female spermatheca (SP) together with Cif proteins, however, neither CifA nor CifB transfer from SP to the uninfected embryos. (iv) In wMel+ ovaries, CifA has nuclear localization, whereas CifB is cytoplasmic before and after blood feeding. (v) Fertilized embryos derived from wMel+ females show CifA localization in the nuclei of early mitotic stage and at the nuclear periphery in the

cytoplasm during late division cycles. (vi) Importantly, there is no colocalization or binding of CifA and CifB in the fertilized embryos.

We detected a few differences in wMel Cifs' localization in the transinfected Ae. aegypti mosquitoes compared to our previous work shown in the natural host of D. melanogaster flies [50]. During pre-meiotic spermatogenesis stage, CifB was not detected in the germ cells in Drosophila, whereas in Ae. aegypti, CifB localizes to the germline cytoplasm. Both CifA and CifB are nuclear in fly spermatocytes but cytoplasmic in mosquitoes. During post-meiosis and elongation stages in flies, CifA and CifB located in the presumed acrosomal region of sperm head. In mosquitoes, CifA exits out of the elongating sperm head and localizes to the cytoplasmic periphery, and CifB decorates the sperm nuclei in a distinct puncta manner. Upon maturation, CifA strictly lies on the sperm tail and CifB occurs with the head in dense puncta form and faint signals along the tail. We hypothesize that the differences in localization in flies and mosquitoes might be due to species-specific differences in sperm morphogenesis or chromatin organization and condensation processes [82,83]. Indeed, to detect Cifs in tightly packaged mature sperm, decondensation of mosquito sperm was not necessary as done previously in flies [50], suggesting that mosquitoes have a less condensed sperm architecture than flies even though they possess the same sperm head diameter [84,85]. These differences may underpin the extent and specifics of the wMel protein—chromatin interactions in different host species.

During the postmeiotic elongation process, sperm chromatin undergoes a dramatic reorganization from a nucleosomal histone-based structure to a protamine-based structure. In accordance with our previous data [50], we here showed that the histone-to-protamine transition occurs abnormally in wMel+ Ae. aegypti. Unlike flies in which retained histones were detected only until elongating late-canoe spermatids [50], punctate histones were detected on the surface of mature mosquito sperm, highlighting once again the species-specificity of wMel protein—chromatin interactions that may be suggestive of variable CI penetrance (fly host, brief histone retention) versus consistently strong CI (mosquito host, long histone retention). We further highlight a 19% higher protamine deficiency levels in mosquitoes that correlates with their high CI levels [23,25,34] compared to flies. The protamine deficiency changes also varied in sperm isolated from females in wMel-Ae. aegypti versus wMel-D. melanogaster. While the CI mechanism generally remains conserved in these host species, there might be additional factors at play, such as CI-related variation in sperm size, length, and species-specific sperm DNA compaction [55,83,84] that may affect which sperm successfully fertilize females. Future comparative investigations on sperm genome architecture, relative nucleoprotamine structural organization, and chromosomal arrangement across insect species will be helpful to determine the underlying factors that may explain varying CI penetrance.

After mating, sperm isolated from the female reproductive tract contained CifA along the tail and CifB decorated the head and tail. Cifs were not detected in the fertilized embryo. There are 2 reasons to explain this result. The first is biological, namely that Cifs are shredded off the sperm surface before embryos are fertilized. Indeed, the plasma membrane of mature sperm in mosquitoes and other animals is covered by a thick glycoprotein coat or glycocalyx [86], which upon mating masks the sperm from an immediate female immune attack [87,88]. Within 24 h of storage in the female reproductive tract, *Ae. aegypti* sperm shed their glycocalyx to become motile for fertilizing the egg [89]. Thus, it is possible that Cifs are removed during glycocalyx processing or degraded before sperm entry into the egg through exocytosis of acrosomal content [90], as we discussed previously [50]. The second reason can be a technical challenge of detecting Cifs as the proteins may not sufficiently stain in embryos perhaps owing to their low abundance. However, since the Cifs are detectable in mature sperm at the same abundance expected inside eggs, this explanation seems unlikely. Moreover, CifA is detectable in rescue

embryos in this study, thus demonstrating that the staining technique works in embryos. Future research may involve experiments with various staining techniques.

Maintaining sperm genomic integrity is important not only for successful fertilization and embryo development, but also to ensure proper transmission of genetic information across generations. During spermatogenesis, replacement of histones by protamines is facilitated by various posttranslational modifications (PTMs). This transition is also the most vulnerable phase of spermatogenesis for the induction of DNA breaks followed by an immediate repair process for regulating chromatin compaction [81,91]. With insufficient PTMs and DNA repair, developing sperm accumulate errors in the epigenome that can transmit to the egg with important implications for the fate of developing embryo [92-94]. Once fertilization occurs, the transferred sperm with an imbalanced protamine content could suffer from remodeling errors in the chromatin structure, leading to DNA breaks that eventually cause chromosometype aberrations [95]. The repair of sperm DNA breaks is a key factor to ensure proper embryo development, especially when paternal DNA integrity is compromised [96–98]. In mice, zygotes recognize and respond to DNA damage derived from sperm by specifically delaying paternal DNA replication, causing defective embryonic development and ultimately developmental arrest [99]. Indeed, protamine removal is unaffected in CI embryos, and it is the paternal DNA replication that is delayed in CI sperm, with retention of proliferating cell nuclear antigen, a replication stress marker [51,100].

Thus, we summarize our cell biological knowledge of CI in light of the Host Modification model (Fig 7), in which wMel Cif proteins in males localize and interact with the developing sperm nucleus. Resultantly, the CI sperm develop with compromised RNA and DNA content [101] and irregular histone retention and protamine deficiency in *D. melanogaster* [50] and *Ae. aegypti* mosquitoes, observed in this study. A disrupted replacement of histones may alter the epigenetic memory of CI sperm that can be inherited to dictate the fate of embryonic development [102,103]. We speculate that post-fertilization, the modified CI sperm with imbalanced protamine content experience chromatin remodeling defects leading to improper condensation and replication errors. These errors eventually cause embryonic developmental arrest and lethality unless rescued by potentially similar epigenetic changes imparted by wMel + females expressing CifA during oogenesis and/or embryogenesis as discussed below. The unmodified sperm from wMel- males will be compatible with embryos derived from either modified (wMel+) or unmodified (wMel-) females because maternal chromatin decides the rate of nuclear mitotic progression [104].

wMel CifA in Ae. aegypti females invade nuclei of germline stem cells, nurse cells, and the oocyte nucleoplasm containing the chromatin mass. These findings are strongly consistent with the nuclear-targeting CifA harboring a functional nuclear localization signal previously reported in fly experiments [50]. Moreover, CifA is biochemically characterized as a RNase [101], and Wolbachia is known to cause oxidative stress in Ae. aegypti ovaries [105]. Therefore, it remains plausible if not likely that wMel CifA in the oocyte nucleus interacts with maternal chromatin and induces changes to ultimately sync with wMel-modified paternal chromatin to rescue CI (Fig 7). Indeed, in mammals, the oocyte is primed to repair genomic integrity of the fertilizing sperm by encoding transcripts that are more abundant in the early embryo than in the later stages [106,107].

After fertilization, no Cif proteins were detected in CI embryos, establishing that paternally encoded, wild-type Cifs are unlikely to transfer to the embryo. It is the fatal paternal genome modification that is necessary to be delivered and manifest CI. Strikingly, we found CifA presence in mosquito embryos derived from *Wolbachia*-infected females where CifA overlaps with nuclei during early mitotic divisions and concentrates in and around the nuclear periphery and in the cytoplasm during later division cycles. While the lack of paternal *w*Mel transgenic

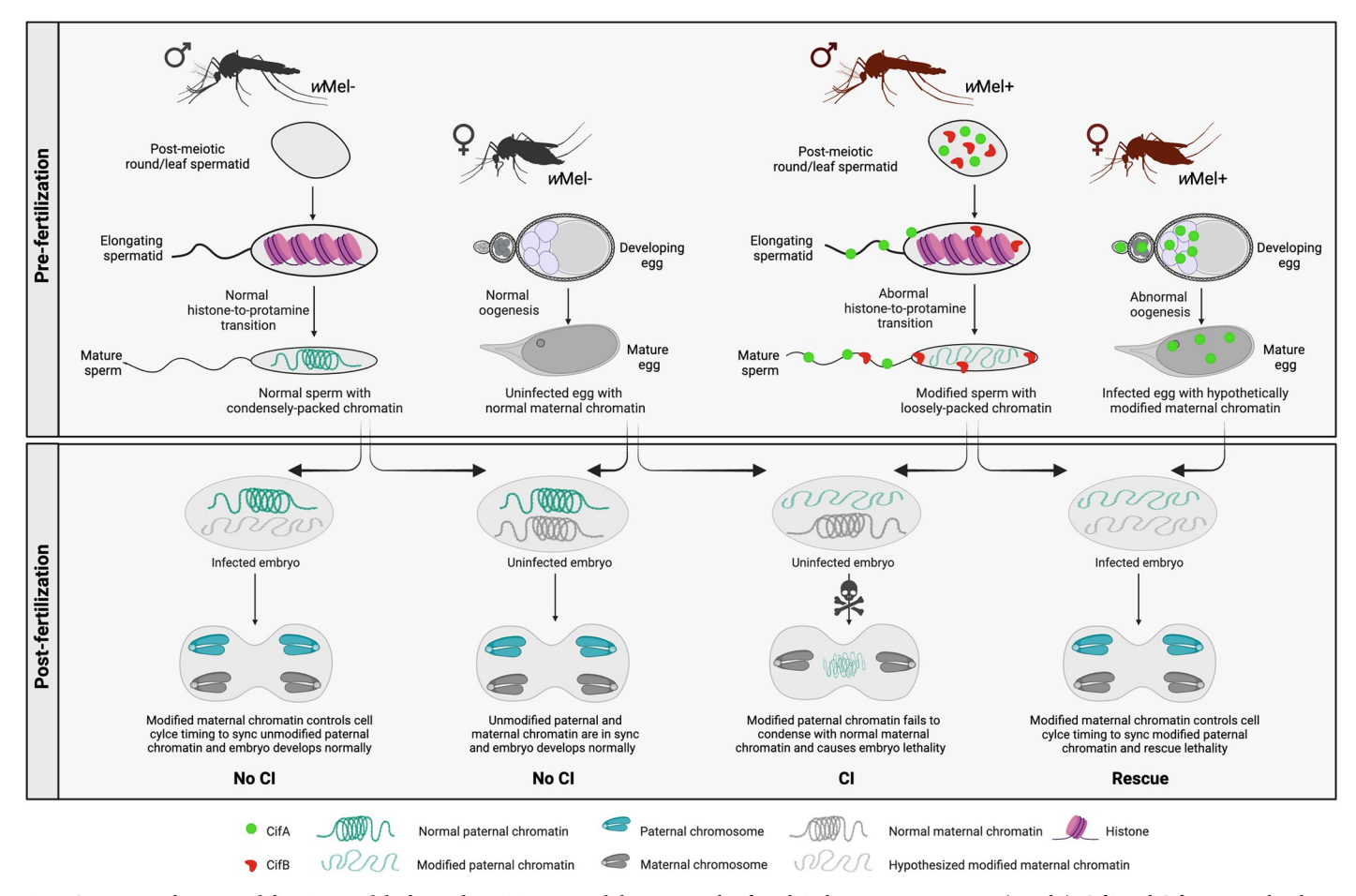


Fig 7. Summary of Host Modification Model of cytoplasmic incompatibility. In wMel-infected Aedes aegypti mosquitoes (wMel+), CifA and CifB proteins localize in postmeiotic spermatid nuclei. Upon elongation and maturation, while CifB resides in the sperm nucleus, CifA exits and localize to sperm tail. During elongation, histones wrapped around spermatid DNA are normally removed and replaced by protamines that bind and tightly package the sperm chromatin for maintaining compact genome integrity. In uninfected mosquitoes (wMel-), histone-to-protamine transition occur normally, whereas in wMel+ males, Cif proteins cause abnormal retention of histones and lack of protamine binding to the DNA. Sperm chromatin integrity altered pre-fertilization results in post-fertilization embryonic catastrophe. Upon fertilizing an uninfected egg, the modified sperm chromatin fails to condense and synchronize with maternal chromatin during early mitotic divisions, causing CI-defining embryonic lethality. However, the unmodified sperm from wMel- males will be compatible with embryos derived from either modified (wMel+) or unmodified (wMel-) females because maternal chromatin decides the rate of nuclear mitotic progression. Image was created with Biorender.com.

and wild-type CifA and CifB transfer is a replicated result across flies and mosquitoes, the presence of CifA in mosquito embryos varies. CifA in flies was only detectable until early oogenesis events; it was absent in embryos [50]. However, in mosquitoes, it is present and affiliated with DNA during early mitotic events of embryogenesis. We speculate that CifA's presence in the oocyte nucleus of mosquito ovaries (and absence in fly oocytes) explains CifA transfer to mosquito embryos. In association with this difference, we also note that the symbiont density, distribution, and expression of *Wolbachia* in new, transinfected hosts can change dramatically, impacting protein expression, localization, and host phenotypes. Indeed, *w*Mel in *Ae. aegypti* is stable and has a higher within-host density [34]. Whether CifA in mosquito embryos is maternally provisioned or embryonically expressed by *Wolbachia* cells requires further investigation. Differential labeling of male versus female pronuclei with specific markers [108] may

potentially establish CifA localization to the female pronucleus if it is maternally derived, or to both pronuclei if *Wolbachia*-derived.

Based on *D. melanogaster* data, we proposed a CifA-mediated Host Modification Model of rescue whereby CifA modifies host factors during oogenesis (a parallel concept to the CI-induced testes modifications) to impart maternal chromatin changes, which then pass down to the zygote for rescue [49,50]. An updated model based on the *Ae. aegypti* data reported here is that CifA proteins can access and/or interact with maternal chromatin not only during oogenesis, but also embryogenesis for maternal chromatin modification to persist and consistently rescue strong CI in this system. Indeed, in murine models, the zygote can repair compromised sperm DNA integrity using maternal DNA repair machinery [109]. However, we caution that it is difficult to test the proximal time and location of the rescue mechanism in a wild-type system where *Wolbachia* are present in both the ovaries and embryos. Transgenic *cif* expression under the control of ovarian- or embryonic-specific expression could, in theory, tease these alternatives apart. In this light, it is noteworthy that transgenic rescue is achieved with diverse CifA variants only by ovarian expression (not embryonic expression) till date [14,49,69,110–112].

Finally, the collective data on wMel CI cellular biology [50] (and this study) in support of Host Modification (HM) model of CI contrasts with that of wPip from Culex pipiens mosquitoes studied in a non-native D. melanogaster host [51]. Our in vivo evidence in both flies and mosquitoes establishes that the CI-defining host modifications incipiently launch prefertilization, and fatal paternal genome modification is delivered to the embryo to manifest CI. CifA_{wMel} and CifB_{wMel} in the sperm very likely do not transfer to the embryos for inducing CI, and CifA_{wMel} and CifB_{wMel} do not bind in the embryos for rescue. On the other hand, another study [51] claims that the transfer of CifB_{wPip} toxin to the fertilized embryo associated with paternal genome replication stress kills embryos. We highlight that the interpretation of this result, while extendable to the premise that CifB causes paternal genome replication errors in the embryo, has an alternative and more parsimonious explanation with the data here. Namely, the integrity of paternal DNA in the embryo is compromised pre-fertilization, which secondarily results in post-fertilization replication stress. This hypothesis was not tested in the study [51]. Additionally, the study predicts that upon fertilization, the maternal CifA_{wPip} should be present in the egg cytoplasm to bind paternally delivered CifB_{wPip} and neutralize its toxicity for rescuing CI. There is no cell biological evidence for this fundamental premise of the toxin-antitoxin model [51]. Notably, the host genotype can regulate induction and/or suppression of CI and rescue [38,113-115]. Therefore, discrepancies in Cif protein transfer and localization could result from a transgenic artifact. For instance, overexpressed, transgenic CifB_{wPip} in a foreign fly host is likely to act aberrantly from wild-type CifB, the latter of which was not measured in embryos from the natural host C. pipiens. Here, using the same wMel strain from native D. melanogaster in non-native Ae. aegypti hosts, we establish that the mechanism of CI in WMP mosquitoes is largely controlled by the Wolbachia strain because histone retention, protamine deficiency, and lack of paternal CifA and/or CifB detection in the embryos are shared facets of CI across both hosts.

CI is the symbiotic drive used by the WMP to rapidly spread *Wolbachia* and replace the wild uninfected *Ae. aegypti* population to reduce their vectorial competence and improve global health. While this work characterizes the long-sought mechanism of CI and its conservation across *D. melanogaster* and *Ae. aegypti*, it also raises the potential for leveraging the altered sperm nucleoprotein composition, if needed, to genetically engineer and optimize CI in vectors or pests that are either refractory to *Wolbachia* infection or lack the capacity for *Wolbachia*-induced CI.

Materials and methods

Mosquito strains

Aedes aegypti mosquito lines with and without wMel Wolbachia infection were obtained from Monash University (wMel) [23] for the majority of the work and subsequently from the University of Melbourne, Australia (wMelM) [24] for the qPCR-based cif expression experiments in embryos (S4 Fig). Both strains induce strong CI with 100% identity in the cifA and cifB gene sequences [24]. The colonies were reared and maintained at Vanderbilt University and Penn State University, USA, in environmental chambers at 27 °C and 75% relative humidity on a 12-h light/dark cycle. Eggs were hatched in water and larvae fed a mixture of Koi food and baker's yeast. Pupae from the wMel+ and wMel- colonies were transferred to six-well plates, and upon eclosion, adults were anesthetized on ice and separated by sex; this procedure prevented mating. Adults were housed in 900 cm3 cages with screen walls and fed 10% sucrose ad libitum. The sexes were maintained separately for experimental purposes.

Immunofluorescence: Testes

Adult virgin mosquito males (4 to 5 days old) with and without *w*Mel were collected for testes dissection in ice-cold 1× PBS solution. Dissected tissues were fixed in 4% formaldehyde diluted in 1× PBS for 30 min at room temperature and washed in PBS-T (1× PBS + 0.3% TritonX-100) 3 times for 5 min each. Tissues were then blocked in 1% BSA in PBS-T (1× PBS + 0.1% TritonX-100) for 1 h at room temperature. They were then incubated independently with primary antibodies: anti-rabbit CifA (1:500), anti-rabbit CifB (1:500), and anti-mouse Histone (1:1,000) (Millipore Sigma, Cat# MABE71) overnight at 4 °C rotating. After washing in PBS-T 3 times for 5 min each at room temperature, tissues were incubated with secondary antibodies: goat anti-rabbit Alexa Fluor 594 secondary antibody (Fisher Scientific, Cat# A11037) and goat anti-mouse Alexa Fluor 488 (Thermo Fisher Scientific, Cat# A11034) at 1:1,000 dilution for 4 h at room temperature in the dark. Tissues were then washed 3 times for 5 min each in PBS-T and mounted in Vectashield mounting media containing DAPI (Vector laboratories, Cat# H120010). Imaging was performed under Zeiss LSM 880 confocal microscope under constant exposure settings.

Sperm isolation and Chromomycin A3 staining

Sperm from seminal vesicles of 4 to 5 days old virgin males with and without wMel were extracted on a microscope slide using forceps and fixed in 3:1 vol/vol methanol:acetic acid at 4 °C for 20 min. Excess solution was then removed, and the slide was air-dried. Each slide was treated in the dark for 20 min with 0.25 mg/ml of CMA3 in McIlvain's buffer (pH 7.0), with 10 mM MgCl₂. Sperm was then washed in 1× PBS, mounted, and imaged using Zeiss LSM 880 confocal microscope. All images were acquired with the same parameters for each line and did not undergo significant alteration. Fluorescence quantification was performed by scoring fluorescent pixels in arbitrary units (A.U.) within individual sperm heads using ImageJ software as per the details described in [116]. Specifically, an area of interest was manually drawn around individual sperm head in both CMA3 and DAPI channels. "Analyze" function was used to measure the area from DAPI channel and raw integrated density (RawIntDen) from CMA3 channel. RawIntDens is the total signal intensity of all the pixels with that particular area that measured fluorescence CMA3 intensity per sperm head. A corrected total cell fluorescence (CTCF) was then calculated by dividing RawIntDens to the area and graphed. The overlapping sperm areas were omitted from the quantification analysis. Statistical significance (p < 0.05) was determined by a pairwise comparison using Mann—Whitney test in GraphPad Prism 10.

Immunofluorescence: Ovaries

Virgin females (4 to 5 days old) with no blood-feeding and 24 h post blood-feeding with and without wMel were dissected to isolate ovaries. Mosquitoes were fed defibrinated sheep blood for 2 h using a Hemotek artificial membrane feeding system heated to 37 °C (Hemotek, Lancashire, UK). Ovaries were dissected in 1× PBS on ice and processed as previously [50]. Tissues were incubated with primary antibodies α -FtsZ (1:150) (a kind gift from Dr. Irene Newton, Indiana University) to stain Wolbachia, α -CifA, and α -CifB (1:500) at 4 °C overnight followed by secondary antibody (Alexa Fluor 594, 1:1,000) for 4 h at room temperature in the dark. Samples were then rinsed and blocked again before incubating at 4 °C overnight. After washing in 1× PBS-T 3 times, samples were incubated with a secondary antibody (Alexa Fluor 594) for 4 h in the dark. Tissues were then washed 3 times for 5 min each in 1× PBS and mounted in Vectashield mounting media containing DAPI (Vector laboratories, Cat# H120010). Imaging was performed with a Zeiss LSM 880 confocal microscope.

Immunofluorescence: Embryos

Embryos with and without *w*Mel were collected 0 to 3 h AED on moist filter paper substrate to capture first and subsequent mitotic division events [68]. To slow down embryogenesis at preselected times, the moist filter paper was briefly held at 4 °C. The embryo bleaching and dechorionation protocol was developed from [117]. Briefly, the exochorion was removed by incubating embryos in 50% bleach for 40 s followed by thorough rinsing with distilled water to remove all traces of bleach. The embryos were then transferred to fixative solution (1:1 4% paraformaldehyde and heptane) in a microcentrifuge tube and incubated in a 60 °C water bath for 30 min. Fixative was removed and replaced with heptane pre-chilled at –80 °C. Embryos were incubated at –80 °C for 5 min. After adding room temperature methanol, embryos vials were vigorously shaken under warm running water for 30 s. The top heptane layer and bottom methanol layer was removed, and embryos were washed 3 to 4 times with fresh methanol to remove residual heptane. Fixed embryos were stored at –20 °C until further use.

Before proceeding to the immunofluorescence assay, the endochorion was manually peeled according to previously established methods [118]. Peeled embryos were then rehydrated with 1× PBS for 5 min followed by 2 times 10 min rinses in 1× PBS-T. Samples were then blocked in 1% BSA in PBS-T for 1 h at room temperature. For samples incubated with 2 primary antibodies generated in different host species, all staining and imaging steps were carried out as for testes and ovary tissues detailed above. For the double-immunolabeling experiments in which the 2 primary antibodies were generated in the same host species (α -CifA and α -CifB in rabbit), we followed previously established protocols [119,120]. Briefly, samples were first incubated with the α-CifA antibody for 1 h at room temperature, rinsed 3 times for 5 min in PBS, and incubated overnight at 4 °C with a DyLight 488-conjugated goat Fab' fragment antirabbit IgG (Jackson ImmunoResearch Laboratories, West Grove, PE, USA) at a 1:100 dilution in PBS. Samples were then rinsed 6 times for 5 min in PBS, incubated with α-CifB for 1 h at room temperature, rinsed 3 times for 5 min in PBS, and then incubated with a goat anti-rabbit Alexa Fluor 594 secondary antibody for 4 h in the dark at room temperature. Samples were then washed 3 times for 5 min each in 1× PBS and mounted in Vectashield mounting media containing DAPI (Vector laboratories, Cat# H120010). Imaging was performed under Zeiss LSM 880 confocal microscope using constant exposure settings.

RNA isolation and qPCR: Embryos

Mosquito embryos with wMelM were collected 0 to 2 h AED on moist filter paper substrate for RNA isolation. The collected samples were immediately manually crushed with RNA-free

pestles (USA Scientific, #1415–5390) in liquid nitrogen. RNA was extracted using the Direct-zol RNA MiniPrep Kit (Zymo) followed by DNase treatment (Ambion, Life Technologies), and 1 μg of total RNA was used to synthesize cDNA with SuperScript VILO kit (Invitrogen, #11755250) and cDNA was diluted 1:10 using Ambion nuclease-free water for use in qPCR. qPCR was performed on a QuantStudio 6 Pro Real-Time PCR system using PowerTrack SYBR Green Mastermix (Applied Biosystems, #A46109) with the following conditions: 50 °C 2 min, 95 °C 10 min, 40× (95 °C 15 s, 60 °C 30 s), 95 °C 15 s, 60 °C 1 min, 95 °C 15 s. *cifA* and *cifB* primers and *Wolbachia*-specific *groEL* gene primers were used as described earlier [14,49]. Each reaction was run in 2 technical replicates. Expressions of *cifA* and *cifB* relative to *groEL* were compared using the 2^{-ΔCt} method. Ct values above 30 were omitted from the analysis.

Supporting information

S1 Fig. CifA occasionally localize to mature sperm in wMel+ males. Cifs are absent in wMel- testes. Testes (n = 10) from 4 to 5 days old males of wild-type wMel+ and wMel- Ae. aegypti were dissected and immunostained to visualize CifA (green) and CifB (red) during sperm morphogenesis. DAPI stain (blue) labeled nuclei. (A) CifA was localized in puncta form to the mature sperm head in 1 out of 10 wMel+ testes examined. (B) Both CifA and CifB signals are absent in wMel- control mosquito testes. The experiment was conducted in parallel to the one shown in Fig 1. (TIF)

S2 Fig. Needle spermatids in wMel+ males abnormally retain histones relative to wMel-ones. wMel+ and wMel- testes (n = 10) from 4 to 5 days old virgin males were dissected and immunostained to visualize and quantify core-histone abundance (magenta) in needle spermatids in Ae. aegypti. DAPI stain (blue) labeled spermatid nuclei. wMel+ males show prolonged histone retention in the form of puncta in condensing needle-stage spermatids, whereas histones are removed in wMel- males as expected. Solid arrow indicates somatic histone signals forming testes with no differentiating signals in wMel+ and wMel- testes, as expected. The dotted arrow shows histones specific to developing sperm under wMel+ infection, which are the subject of this study. The images are related to needle spermatid data shown in Fig 2. (TIF)

S3 Fig. CifA localizes in and around the nuclei in rescue embryos. Related to Fig 4, CifA localizes with nuclear DNA and surrounding cytoplasm of 8 daughter cells in rescue embryos collected at approximately 2 h AED during nuclear cycle 3. Upon higher exposure of DAPI channel in gray, the top panel shows there is an embedded nucleus (indicated by white arrow) of another daughter cell that surfaces in a different z-plane as shown in the bottom panel. (TIF)

S4 Fig. *cifA* gene expression is approximately 10-fold higher than *cifB* in early *Ae. aegypti* embryos. Embryos from *w*MelM *Wolbachia* strain aged 0–2 h AED were tested for gene expression analysis of *cifA* and *cifB* relative to *Wolbachia groEL* gene. Horizontal bars represent median value. Statistical significance (p < 0.05) was determined by running pairwise comparisons based on Mann—Whitney U test. All the *p*-values are reported in S1 Table. Raw data underlying this figure can be found in S1 Data file. (TIF)

S5 Fig. Cifs and *Wolbachia* are absent in *w*Mel- ovaries. (A, B) Immunostaining assay shows that during both pre- (A) and post- (B) blood feeding, *w*Mel- ovaries are devoid of any *Wolbachia* (red), CifA (green), and CifB (yellow) signals, as expected. The experiment was conducted in parallel to the one shown in Fig 6. We note autofluorescence observed in red, green, and yellow channels outlining the tissue morphology does not signify *Wolbachia*, CifA, and CifB signals, respectively.

S6 Fig. CifA occasionally localizes to nurse cell nuclei. Immunostaining assay shows that in non-blood fed *w*Mel+ females, CifA (in green) localize in the nuclei of germarium (ger), nurse cells (arrowheads), and oocyte (oo). Within the oocyte, CifA is present in the oocyte nucleus (on) inhabiting nucleoplasm space containing chromatin mass (ch) and a nucleolus (no). CifA colocalizes with chromatin outside of the nucleolus area. (TIF)

S1 Table. *P*-values associated with all statistical comparisons made for quantification data. (XLSX)

S1 Data. Raw metadata underlying figures. (XLSX)

Acknowledgments

(TIF)

We are grateful to Dr. Scott O'Neill (Monash University) for providing mosquito colonies used in the World Mosquito program for this experimental study and comments on earlier versions of the manuscript. We thank Dr. Benjamin Loppin (ENS de Lyon, France) and Dr. Irene Newton (Indiana University, USA) for providing useful feedback on the immunostaining protocol, Heather Engler (Penn State University); Ary Hoffmann, Perran Ross, and Xinyue Gu (PEARG group, Bio21 Institute at the University of Melbourne) for rearing mosquitoes used in the embryo qPCR experiment; the Cell Imaging Shared Resource (Vanderbilt University); and the shared microscopy facility at the Huck Institute of Life Sciences (Penn State University) for imaging assistance. We thank Sarah Bordenstein and members of the Bordenstein lab for providing helpful feedback on the manuscript.

Author Contributions

Conceptualization: Rupinder Kaur, Seth R. Bordenstein.

Data curation: Rupinder Kaur. **Formal analysis:** Rupinder Kaur.

Funding acquisition: Seth R. Bordenstein. **Investigation:** Rupinder Kaur, Cole J. Meier.

Methodology: Rupinder Kaur, Cole J. Meier, Julian F. Hillyer, Seth R. Bordenstein.

Project administration: Seth R. Bordenstein.

Resources: Elizabeth A. McGraw, Julian F. Hillyer, Seth R. Bordenstein.

Supervision: Rupinder Kaur, Julian F. Hillyer, Seth R. Bordenstein.

Validation: Rupinder Kaur, Seth R. Bordenstein.

Visualization: Rupinder Kaur.

Writing - original draft: Rupinder Kaur.

Writing – review & editing: Rupinder Kaur, Cole J. Meier, Elizabeth A. McGraw, Julian F. Hillyer, Seth R. Bordenstein.

References

- Ricci I, Valzano M, Ulissi U, Epis S, Cappelli A, Favia G. Symbiotic control of mosquito borne disease. Pathog Glob Health. 2012; 106:380–385. https://doi.org/10.1179/2047773212Y.0000000051 PMID: 23265608
- Teixeira L, Ferreira Á, Ashburner M. The bacterial symbiont Wolbachia induces resistance to RNA viral infections in Drosophila melanogaster. PLoS Biol. 2008; 6:2753–2763. https://doi.org/10.1371/journal.pbio.1000002 PMID: 19222304
- Hedges LM, Brownlie JC, O'Neill SL, Johnson KN. Wolbachia and Virus Protection in Insects. Science. 1979; 2008(322):702–702. https://doi.org/10.1126/science.1162418 PMID: 18974344
- Moreira LA, Iturbe-Ormaetxe I, Jeffery JA, Lu G, Pyke AT, Hedges LM, et al. A Wolbachia symbiont in Aedes aegypti limits infection with dengue, Chikungunya, and Plasmodium. Cell. 2009; 139:1268– 1278. https://doi.org/10.1016/j.cell.2009.11.042 PMID: 20064373
- van den Hurk AF, Hall-Mendelin S, Pyke AT, Frentiu FD, McElroy K, Day A, et al. Impact of Wolbachia on Infection with Chikungunya and Yellow Fever Viruses in the Mosquito Vector Aedes aegypti. PLoS Negl Trop Dis. 2012: 6. https://doi.org/10.1371/journal.pntd.0001892 PMID: 23133693
- Caragata E, Dutra H, Moreira L. Inhibition of Zika virus by Wolbachia in Aedes aegypti. Microbial Cell. 2016; 3:293–295. https://doi.org/10.15698/mic2016.07.513 PMID: 28357366
- Bian G, Xu Y, Lu P, Xie Y, Xi Z. The Endosymbiotic Bacterium Wolbachia Induces Resistance to Dengue Virus in Aedes aegypti. PLoS Pathog. 2010; 6:e1000833. https://doi.org/10.1371/journal.ppat.1000833 PMID: 20368968
- Terradas G, McGraw EA. Wolbachia-mediated virus blocking in the mosquito vector Aedes aegypti. Curr Opin Insect Sci. 2017; 22:37–44. https://doi.org/10.1016/j.cois.2017.05.005 PMID: 28805637
- Bhattacharya T, Newton ILG, Hardy RW. Viral RNA is a target for Wolbachia-mediated pathogen blocking. PLoS Pathog. 2020. https://doi.org/10.1371/journal.ppat.1008513 PMID: 32555677
- Shropshire J, Leigh B, Bordenstein SR, Initiative M. Symbiont-mediated cytoplasmic incompatibility: What have we learned in 50 years? Elife. 2020:1–51. https://doi.org/10.7554/eLife.61989 PMID: 32975515
- Breeuwer JAJ, Werren JH. Microorganisms associated with chromosome destruction and reproductive isolation between two insect species. Nature. 1990. https://doi.org/10.1038/346558a0 PMID: 2377229
- Callaini G, Riparbelli MG, Giordano R, Dallai R. Mitotic defects associated with cytoplasmic incompatibility in Drosophila simulans. J Invertebr Pathol. 1996; 67:55–64. https://doi.org/10.1006/jipa. 1996.0009
- Lassy CW, Karr TL. Cytological analysis of fertilization and early embryonic development in incompatible crosses of Drosophila simulans. Mech Dev. 1996; 57:47–58. https://doi.org/10.1016/0925-4773 (96)00527-8 PMID: 8817452
- LePage DP, Metcalf JA, Bordenstein SR, On J, Perlmutter JI, Shropshire JD, et al. Prophage WO genes recapitulate and enhance Wolbachia-induced cytoplasmic incompatibility. Nature. 2017; 543:243–247. https://doi.org/10.1038/nature21391 PMID: 28241146
- Reed KM, Werren JH. Induction of paternal genome loss by the paternal-sex-ratio chromosome and cytoplasmic incompatibility bacteria (Wolbachia): A comparative study of early embryonic events. Mol Reprod Dev. 1995. https://doi.org/10.1002/mrd.1080400404 PMID: 7598906
- Ryan SL, Saul GB. Post-fertilization effect of incompatibility factors in Mormoniella. Mol Gen Genet. 1968; 103:29–36. https://doi.org/10.1007/BF00271154 PMID: 5753233
- Tram U, Fredrick K, Werren JH, Sullivan W. Paternal chromosome segregation during the first mitotic division determines Wolbachia-induced cytoplasmic incompatibility phenotype. J Cell Sci. 2006; 119:3655–3663. https://doi.org/10.1242/jcs.03095 PMID: 16912076
- Warecki B, Titen SWA, Alam MS, Vega G, Lemseffer N, Hug K, et al. Wolbachia action in the sperm produces developmentally deferred chromosome segregation defects during the Drosophila mid-blastula transition. Elife. 2022: 11. https://doi.org/10.7554/eLife.81292 PMID: 36149408
- Turelli M, Hoffmann AA. Rapid spread of an inherited incompatibility factor in California Drosophila.
 Nature. 1991; 353:440–442. https://doi.org/10.1038/353440a0 PMID: 1896086

- Turelli M. Evolution of incompatibility-inducing microbes and their hosts. Evolution (N Y). 1994;
 48:1500–1513. https://doi.org/10.1111/j.1558-5646.1994.tb02192.x PMID: 28568404
- Weinert LA, Araujo-Jnr EV, Ahmed MZ, Welch JJ. The incidence of bacterial endosymbionts in terrestrial arthropods. Proc Biol Sci. 2015; 282:20150249–20150249. https://doi.org/10.1098/rspb.2015.
 0249 PMID: 25904667
- Zug R, Hammerstein P. Still a host of hosts for Wolbachia: Analysis of recent data suggests that 40% of terrestrial arthropod species are infected. PLoS ONE. 2012: 7. https://doi.org/10.1371/journal.pone.0038544 PMID: 22685581
- Walker T, Johnson PH, Moreira LA, Iturbe-Ormaetxe I, Frentiu FD, McMeniman CJ, et al. The wMel Wolbachia strain blocks dengue and invades caged Aedes aegypti populations. Nature. 2011; 476:450–455. https://doi.org/10.1038/nature10355 PMID: 21866159
- 24. Gu X, Ross PA, Rodriguez-Andres J, Robinson KL, Yang Q, Lau M, et al. A w Mel Wolbachia variant in Aedes aegypti from field-collected Drosophila melanogaster with increased phenotypic stability under heat stress. Environ Microbiol. 2022; 24:2119–2135. https://doi.org/10.1111/1462-2920.15966 PMID: 35319146
- 25. Hoffmann AA, Montgomery BL, Popovici J, Iturbe-Ormaetxe I, Johnson PH, Muzzi F, et al. Successful establishment of Wolbachia in Aedes populations to suppress dengue transmission. Nature. 2011; 476:454–457. https://doi.org/10.1038/nature10356 PMID: 21866160
- Flores HA, O'Neill SL. Controlling vector-borne diseases by releasing modified mosquitoes. Nat Rev Microbiol. 2018; 16:508–518. https://doi.org/10.1038/s41579-018-0025-0 PMID: 29777177
- Gesto JSM, Pinto SB, Dias FBS, Peixoto J, Costa G, Kutcher S, et al. Large-Scale Deployment and Establishment of Wolbachia Into the Aedes aegypti Population in Rio de Janeiro, Brazil. Front Microbiol. 2021: 12. https://doi.org/10.3389/fmicb.2021.711107 PMID: 34394061
- Hoffmann AA, Iturbe-Ormaetxe I, Callahan AG, Phillips BL, Billington K, Axford JK, et al. Stability of the wMel Wolbachia Infection following Invasion into Aedes aegypti Populations. PLoS Negl Trop Dis. 2014. https://doi.org/10.1371/journal.pntd.0003115 PMID: 25211492
- Utarini A, Indriani C, Ahmad RA, Tantowijoyo W, Arguni E, Ansari MR, et al. Efficacy of Wolbachiainfected mosquito deployments for the control of dengue. N Engl J Med. 2021. https://doi.org/10.1056/ NEJMoa2030243 PMID: 34107180
- Indriani C, Tantowijoyo W, Rancès E, Andari B, Prabowo E, Yusdi D, et al. Reduced Dengue Incidence Following Deployments of Wolbachia-Infected Aedes aegypti in Yogyakarta, Indonesia. SSRN Electron J. 2020. https://doi.org/10.2139/ssrn.3544812
- Joubert DA, Walker T, Carrington LB, De Bruyne JT, Kien DHT, Hoang NLT, et al. Establishment of a Wolbachia Superinfection in Aedes aegypti Mosquitoes as a Potential Approach for Future Resistance Management. PLoS Pathog. 2016; 12:1–19. https://doi.org/10.1371/journal.ppat.1005434 PMID: 26891349
- Nazni WA, Hoffmann AA, NoorAfizah A, Cheong YL, Mancini MV, Golding N, et al. Establishment of Wolbachia Strain wAlbB in Malaysian Populations of Aedes aegypti for Dengue Control. Curr Biol. 2019. https://doi.org/10.1016/j.cub.2019.11.007 PMID: 31761702
- Ryan PA, Turley AP, Wilson G, Hurst TP, Retzki K, Brown-Kenyon J, et al. Establishment of wMel Wolbachia in Aedes aegypti mosquitoes and reduction of local dengue transmission in Cairns and surrounding locations in northern Queensland, Australia. Gates Open Res. 2020. https://doi.org/10.12688/gatesopenres.13061.2 PMID: 31667465
- Ross PA, Robinson KL, Yang Q, Callahan AG, Schmidt TL, Axford JK, et al. A decade of stability for wMel Wolbachia in natural Aedes aegypti populations. PLoS Pathog. 2022: 18. https://doi.org/10.1371/journal.ppat.1010256 PMID: 35196357
- Shropshire JD, Hamant E, Cooper BS. Male Age and Wolbachia Dynamics: Investigating How Fast and Why Bacterial Densities and Cytoplasmic Incompatibility Strengths Vary. MBio. 2021: 12. https://doi.org/10.1128/mBio.02998-21 PMID: 34903056
- 36. Calvitti M, Marini F, Desiderio A, Puggioli A, Moretti R. Wolbachia density and cytoplasmic incompatibility in Aedes albopictus: Concerns with using artificial Wolbachia infection as a vector suppression tool. PLoS ONE. 2015: 10. https://doi.org/10.1371/journal.pone.0121813 PMID: 25812130
- Reynolds KT, Thomson LJ, Hoffmann AA. The effects of host age, host nuclear background and temperature on phenotypic effects of the virulent Wolbachia a strain popcorn in Drosophila melanogaster. Genetics. 2003; 164:1027–1034. https://doi.org/10.1126/science.8511587 PMID: 8511587
- 38. Reynolds KT, Hoffmann AA. Male age, host effects and the weak expression or non-expression of cytoplasmic incompatibility in Drosophila strains infected by maternally transmitted Wolbachia. Genet Res (Camb). 2002; 80:79–87. https://doi.org/10.1017/s0016672302005827 PMID: 12534211

- Yamada R, Floate KD, Riegler M, O'Neill SL. Male development time influences the strength of Wolbachia -induced cytoplasmic incompatibility expression in Drosophila melanogaster. Genetics. 2007; 177:801–808. https://doi.org/10.1534/genetics.106.068486 PMID: 17660578
- Ritchie IT, Needles KT, Leigh BA, Kaur R, Bordenstein SR. Transgenic cytoplasmic incompatibility persists across age and temperature variation in Drosophila melanogaster. iScience. 2022; 25:105327. https://doi.org/10.1016/j.isci.2022.105327 PMID: 36304111
- Bordenstein SR, Bordenstein SR. Temperature affects the tripartite interactions between bacteriophage WO, Wolbachia, and cytoplasmic incompatibility. PLoS ONE. 2011: 6. https://doi.org/10.1371/ journal.pone.0029106 PMID: 22194999
- Ross PA, Axford JK, Yang Q, Staunton KM, Ritchie SA, Richardson KM, et al. Heatwaves cause fluctuations in wMel Wolbachia densities and frequencies in aedes aegypti. PLoS Negl Trop Dis. 2020; 14:1–18. https://doi.org/10.1371/journal.pntd.0007958 PMID: 31971938
- 43. Nasehi SF, Fathipour Y, Asgari S, Mehrabadi M. Environmental Temperature, but Not Male Age, Affects Wolbachia and Prophage WO Thereby Modulating Cytoplasmic Incompatibility in the Parasitoid Wasp, Habrobracon Hebetor. Microb Ecol. 2022; 83:482–491. https://doi.org/10.1007/s00248-021-01768-x PMID: 33969432
- **44.** Clark ME, Veneti Z, Bourtzis K, Karr TL. Wolbachia distribution and cytoplasmic incompatibility during sperm development: the cyst as the basic cellular unit of CI expression. 2003; 120:185–198.
- Layton EM, On J, Perlmutter JI, Bordenstein SR, Shropshire JD. Paternal grandmother age affects the strength of Wolbachia-induced cytoplasmic incompatibility in Drosophila melanogaster. MBio. 2019: 10. https://doi.org/10.1128/mBio.01879-19 PMID: 31690673
- 46. Merçot H, Charlat S. Wolbachia infections in Drosophila melanogaster and D. simulans: Polymorphism and levels of cytoplasmic incompatibility. Genetica. 2004:51–59. https://doi.org/10.1023/b:gene. 0000017629.31383.8f PMID: 15088646
- 47. Chafee ME, Zecher CN, Gourley ML, Schmidt VT, Chen JH, Bordenstein SR, et al. Decoupling of host-symbiont-phage coadaptations following transfer between insect species. Genetics. 2011; 187:203–215. https://doi.org/10.1534/genetics.110.120675 PMID: 20944019
- Shropshire JD, On J, Layton EM, Zhou H, Bordenstein SR. One prophage WO gene rescues cytoplasmic incompatibility in Drosophila melanogaster. Proc Natl Acad Sci U S A. 2018; 115:4987–4991. https://doi.org/10.1073/pnas.1800650115 PMID: 29686091
- **49.** Shropshire JD, Bordenstein SR. Two-by-one model of cytoplasmic incompatibility: Synthetic recapitulation by transgenic expression of cifa and cifb in drosophila. PLoS Genet. 2019: 15. https://doi.org/10.1371/journal.pgen.1008221 PMID: 31242186
- 50. Kaur R, Leigh BA, Ritchie IT, Bordenstein SR. The Cif proteins from Wolbachia prophage WO modify sperm genome integrity to establish cytoplasmic incompatibility. PLoS Biol. 2022: 20. https://doi.org/ 10.1371/journal.pbio.3001584 PMID: 35609042
- Horard B, Terretaz K, Gosselin-Grenet A-S, Sobry H, Sicard M, Landmann F, et al. Paternal transmission of the Wolbachia CidB toxin underlies cytoplasmic incompatibility. Curr Biol. 2022. https://doi.org/10.1016/j.cub.2022.01.052 PMID: 35134330
- 52. Harumoto T, Fukatsu T. Perplexing dynamics of Wolbachia proteins for cytoplasmic incompatibility. PLoS Biol. 2022: 20. https://doi.org/10.1371/journal.pbio.3001644 PMID: 35613073
- 53. Wang W, Cui W, Yang H. Toward an accurate mechanistic understanding of Wolbachia-induced cyto-plasmic incompatibility. Environ Microbiol. 2022. https://doi.org/10.1111/1462-2920.16125 PMID: 35859330
- 54. Wandall A. Ultrastructural organization of spermatocysts in the testes of Aedes aegypti (Diptera: Culicidae). J Med Entomol. 1986; 23:374–379. https://doi.org/10.1093/jmedent/23.4.374 PMID: 3735341
- **55.** Clements AN. The Biology of Mosquitoes. Volume 1. Development, Nutrition and Reproduction. 2000.
- 56. Rathke C, Baarends WM, Awe S, Renkawitz-Pohl R. Chromatin dynamics during spermiogenesis. Biochim Biophys Acta Gene Regul Mech. 2014; 1839:155–168. https://doi.org/10.1016/j.bbagrm. 2013.08.004 PMID: 24091090
- 57. Awe S, Renkawitz-Pohl R. Histone H4 Acetylation is Essential to Proceed from a Histone- to a Protamine-based Chromatin Structure in Spermatid Nuclei of Drosophila melanogaster. Syst Biol Reprod Med. 2010; 56:44–61. https://doi.org/10.3109/19396360903490790 PMID: 20170286
- Cho C, Jung-Ha H, Willis WD, Goulding EH, Stein P, Xu Z, et al. Protamine 2 deficiency leads to sperm DNA damage and embryo death in mice. Biol Reprod. 2003; 69:211–217. https://doi.org/10.1095/biolreprod.102.015115 PMID: 12620939

- Bonilla E, Xu EY. Identification and characterization of novel mammalian spermatogenic genes conserved from fly to human. Mol Hum Reprod. 2008; 14:137–142. https://doi.org/10.1093/molehr/gan002 PMID: 18256174
- Baxevanis AD, Landsman D. Histone sequence database: A compilation of highly-conserved nucleoprotein sequences. Nucleic Acids Res. 1996; 24:245–247. https://doi.org/10.1093/nar/24.1.245 PMID: 8594591
- Lolis D, Georgiou I, Syrrou M, Zikopoulos K, Konstantelli M, Messinis I. Chromomycin A3-staining as an indicator of protamine deficiency and fertilization. Int J Androl. 1996; 19:23–27. https://doi.org/10. 1111/j.1365-2605.1996.tb00429.x PMID: 8698534
- 62. Pascini TV, Ramalho-Ortigão M, Martins GF. Morphological and morphometrical assessment of sper-mathecae of aedes aegypti females. Mem Inst Oswaldo Cruz. 2012; 107:705–712. https://doi.org/10.1590/s0074-02762012000600001 PMID: 22990957
- 63. Tram U, Sullivan W. Role of delayed nuclear envelope breakdown and mitosis in Wolbachia-induced cytoplasmic incompatibility. Science. 1979; 2002(296):1124–1126. https://doi.org/10.1126/science. 1070536 PMID: 12004132
- **64.** Callaini G, Dallai R, Riparbelli MG. Wolbachia-induced delay of paternal chromatin condensation does not prevent maternal chromosomes from entering anaphase in incompatible crosses of Drosophila simulans. J Cell Sci. 1997; 110(Pt 2):271–280.
- 65. Bonneau M, Landmann F, Labbé P, Justy F, Weill M, Sicard M. The cellular phenotype of cytoplasmic incompatibility in Culex pipiens in the light of cidB diversity. PLoS Pathog. 2018: 14. https://doi.org/10. 1371/journal.ppat.1007364 PMID: 30321239
- Duron O, Weill M. Wolbachia infection influences the development of Culex pipiens embryo in incompatible crosses. Heredity (Edinb). 2006; 96:493–500. https://doi.org/10.1038/sj.hdy.6800831 PMID: 16639421
- **67.** Wright JD, Barr AR. Wolbachia and the normal and incompatible eggs of Aedes polynesiensis (Diptera: Culicidae). J Invertebr Pathol. 1981; 38:409–418. https://doi.org/10.1016/0022-2011(81)90109-9
- 68. Raminani LN, Cupp EW. Early embryology of Aedes aegypti (L.) (Diptera: Culicidae). Int J Insect Morphol Embryol. 1975; 4:517–528. https://doi.org/10.1016/0020-7322(75)90028-8
- Adams KL, Abernathy DG, Willett BC, Selland EK. Wolbachia cifB induces cytoplasmic incompatibility in the malaria mosquito. 2021. https://doi.org/10.1101/2021.04.20.440637
- 70. Laurence BR. Ovary development in mosquitoes: a review. 1977.
- Valzania L, Mattee MT, Strand MR, Brown MR. Blood feeding activates the vitellogenic stage of oogenesis in the mosquito Aedes aegypti through inhibition of glycogen synthase kinase 3 by the insulin and TOR pathways. Dev Biol. 2019; 454:85–95. https://doi.org/10.1016/j.ydbio.2019.05.011 PMID: 31153832
- 72. Raikhel AS, Dhadialla TS. Accumulation of yolk proteins in insect oocytes. Annu Rev Entomol. 1992; 37:217–251. https://doi.org/10.1146/annurev.en.37.010192.001245 PMID: 1311540
- 73. Gulia-Nuss M, Robertson AE, Brown MR, Strand MR. Insulin-like peptides and the target of rapamycin pathway coordinately regulate blood digestion and egg maturation in the mosquito Aedes aegypti. PLoS ONE. 2011: 6. https://doi.org/10.1371/journal.pone.0020401 PMID: 21647424
- Vital W, Rezende GL, Abreu L, Moraes J, Lemos FJ, Vaz IDS, et al. Germ band retraction as a landmark in glucose metabolism during Aedes aegypti embryogenesis. BMC Dev Biol. 2010: 10. https:// doi.org/10.1186/1471-213X-10-25 PMID: 20184739
- Fiil A. Structural and functional modifications of the nucleus during oogenesis in the mosquito Aedes aegypti. J Cell Sci. 1974; 14:51–67. https://doi.org/10.1242/jcs.14.1.51 PMID: 4856243
- Roth TF, Porter KR. Yolk Protein Uptake in the Oocyte of the Mosquito Aedes Aegypti. L J Cell Biol. 1964; 20:313–332. https://doi.org/10.1083/jcb.20.2.313 PMID: 14126875
- Telfer WH. The Mechanism and Control of Yolk Formation. Annu Rev Entomol. 1965; 10:161–184. https://doi.org/10.1146/annurev.en.10.010165.001113
- Zimowska G, Shirk PD, Silhacek DL, Shaaya E. Vitellin and formation of yolk spheres in vitellogenic follicles of the moth, Plodia interpunctella. Arch Insect Biochem Physiol. 1995; 29:71–85. https://doi. org/10.1002/arch.940290107
- Dearden PK. Germ cell development in the Honeybee (Apis mellifera); Vasa and Nanos expression. BMC Dev Biol. 2006: 6. https://doi.org/10.1186/1471-213X-6-6 PMID: 16503992
- 80. Li T, Hong X, Gong J, Li Y, Li T, Liang Y, et al. Stable Introduction of Plant-Virus-Inhibiting Wolbachia into Planthoppers for Rice Protection. Curr Biol. 2020. https://doi.org/10.1016/j.cub.2020.09.033 PMID: 33035486

- 81. Rathke C, Baarends WM, Jayaramaiah-Raja S, Bartkuhn M, Renkawitz R, Renkawitz-Pohl R. Transition from a nucleosome-based to a protamine-based chromatin configuration during spermiogenesis in Drosophila. J Cell Sci. 2007; 120:1689–1700. https://doi.org/10.1242/jcs.004663 PMID: 17452629
- 82. Ribas-Maynou J, Garcia-Bonavila E, Hidalgo CO, Catalán J, Miró J, Yeste M. Species-Specific Differences in Sperm Chromatin Decondensation Between Eutherian Mammals Underlie Distinct Lysis Requirements. Front Cell Dev Biol. 2021: 9. https://doi.org/10.3389/fcell.2021.669182 PMID: 33996825
- 83. Kasinsky HE, Gowen BE, Ausió J. Spermiogenic chromatin condensation patterning in several hexapods may involve phase separation dynamics by spinodal decomposition or microemulsion inversion (nucleation). Tissue Cell. 2021: 73. https://doi.org/10.1016/j.tice.2021.101648 PMID: 34537592
- 84. Degner EC, Harrington LC. A mosquito sperm's journey from male ejaculate to egg: Mechanisms, molecules, and methods for exploration. Mol Reprod Dev. 2016; 83:897–911. https://doi.org/10.1002/mrd.22653 PMID: 27147424
- 85. Clements AN, Potter SA. The fine structure of the spermathecae and their ducts in the mosquito Aedes aegypti. J Insect Physiol. 1967; 13:1825–1836. https://doi.org/10.1016/0022-1910(67)90018-2 PMID: 6081062
- 86. Ndiaye M, Mattei X, Thiaw OT. Maturation of mosquito spermatozoa during their transit throughout the male and female reproductive systems. Tissue Cell. 1997; 29:675–678. https://doi.org/10.1016/s0040-8166(97)80043-2 PMID: 18627833
- 87. Yudin AI, Treece CA, Tollner TL, Overstreet JW, Cherr GN. The carbohydrate structure of DEFB126, the major component of the cynomolgus macaque sperm plasma membrane glycocalyx. J Membr Biol. 2005; 207:119–129. https://doi.org/10.1007/s00232-005-0806-z PMID: 16550483
- **88.** Toshimori K, Araki S, Öra C, Eddy EM. Loss of sperm surface sialic acid induces phagocytosis: An assay with a monoclonal antibody T21, which recognizes a 54K sialoglycoprotein. Syst Biol Reprod Med. 1991; 27:79–86. https://doi.org/10.3109/01485019108987656 PMID: 1953200
- 89. Noble JM, Degner EC, Harrington LC, Kourkoutis LF. Cryo-Electron Microscopy Reveals That Sperm Modification Coincides with Female Fertility in the Mosquito Aedes aegypti. Sci Rep. 2019: 9. https://doi.org/10.1038/s41598-019-54920-6 PMID: 31811199
- Degrugillier ME, Leopold RA. Ultrastructure of sperm penetration of house fly eggs. J Ultrasruct Res. 1976; 56:312–325. https://doi.org/10.1016/s0022-5320(76)90006-x PMID: 986479
- McPherson S, Longo FJ. Chromatin structure-function alterations during mammalian spermatogenesis: DNA nicking and repair in elongating spermatids. Eur J Histochem. 1993; 37:109–128. PMID: 7688597
- 92. Marchetti F, Bishop JB, Cosentino L, Moore D, Wyrobek AJ. Paternally Transmitted Chromosomal Aberrations in Mouse Zygotes Determine Their Embryonic Fate. Biol Reprod. 2004; 70:616–624. https://doi.org/10.1095/biolreprod.103.023044 PMID: 14585809
- Marchetti F, Wyrobek AJ. Mechanisms and consequences of paternally-transmitted chromosomal abnormalities. Birth Defects Res C Embryo Today. 2005; 75:112–129. https://doi.org/10.1002/bdrc.20040 PMID: 16035041
- 94. Aitken RJ, Baker MA. Causes and consequences of apoptosis in spermatozoa; contributions to infertility and impacts on development. Int J Dev Biol. 2013; 57:265–272. https://doi.org/10.1387/ijdb.130146ja.pmlD; 23784837
- 95. Nasr-Esfahani MH, Salehi M, Razavi S, Anjomshoa M, Rozbahani S, Moulavi F, et al. Effect of sperm DNA damage and sperm protamine deficiency on fertilization and embryo development post-ICSI. Reprod Biomed Online. 2005; 11:198–205. https://doi.org/10.1016/s1472-6483(10)60959-5 PMID: 16168218
- **96.** Evenson DP, Darzynkiewicz Z, Melamed MR. Relation of mammalian sperm chromatin heterogeneity to fertility. Science. 1979; 1980(210):1131–1133. https://doi.org/10.1126/science.7444440 PMID: 7444440
- **97.** Derijck A, van der Heijden G, Giele M, Philippens M, De boer P. DNA double-strand break repair in parental chromatin of mouse zygotes, the first cell cycle as an origin of de novo mutation. Hum Mol Genet. 2008; 17:1922–1937. https://doi.org/10.1093/hmg/ddn090 PMID: 18353795
- Ménézo Y, Dale B, Cohen M. DNA damage and repair in human oocytes and embryos: A review.
 Zygote. 2010; 18:357–365. https://doi.org/10.1017/S0967199410000286 PMID: 20663262
- Gawecka JE, Marh J, Ortega M, Yamauchi Y, Ward MA, Ward WS. Mouse Zygotes Respond to Severe Sperm DNA Damage by Delaying Paternal DNA Replication and Embryonic Development. PLoS ONE. 2013: 8. https://doi.org/10.1371/journal.pone.0056385 PMID: 23431372
- 100. Landmann F, Orsi GA, Loppin B, Sullivan W. Wolbachia-mediated cytoplasmic incompatibility is associated with impaired histone deposition in the male pronucleus. PLoS Pathog. 2009: 5. https://doi.org/10.1371/journal.ppat.1000343 PMID: 19300496

- Kaur R, McGarry A, Shropshire JD, Leigh BA, Bordenstein SR. Prophage proteins alter long noncoding RNA and DNA of developing sperm to induce a paternal-effect lethality. Science. 2024; 383 (6687):1111–1117. https://doi.org/10.1126/science.adk9469 PMID: 38452081
- 102. Jenkins TG, Carrell DT. Dynamic alterations in the paternal epigenetic landscape following fertilization. Front Genet. 2012: 3. https://doi.org/10.3389/fgene.2012.00143 PMID: 23024648
- 103. Jenkins TG, Carrell DT. The sperm epigenome and potential implications for the developing embryo. Reproduction. 2012; 143:727–734. https://doi.org/10.1530/REP-11-0450 PMID: 22495887
- 104. Ferree PM, Sullivan W. A genetic test of the role of the maternal pronucleus in Wolbachia-induced cytoplasmic incompatibility in Drosophila melanogaster. Genetics. 2006; 173:839–847. https://doi.org/10.1534/genetics.105.053272 PMID: 16624919
- 105. Pan X, Zhou G, Wu J, Bian G, Lu P, Raikhel AS, et al. Wolbachia induces reactive oxygen species (ROS)-dependent activation of the Toll pathway to control dengue virus in the mosquito Aedes aegypti. Proc Natl Acad Sci U S A. 2012; 109:E23–E31. https://doi.org/10.1073/pnas.1116932108 PMID: 22123956
- 106. Ashwood-Smith MJ, Edwards RG. DNA repair by oocytes. Mol Hum Reprod. 1996; 2:46–51. https://doi.org/10.1093/molehr/2.1.46 PMID: 9238657
- 107. Zeng F, Baldwin DA, Schultz RM. Transcript profiling during preimplantation mouse development. Dev Biol. 2004; 272:483–496. https://doi.org/10.1016/j.ydbio.2004.05.018 PMID: 15282163
- 108. Bonneau M, Landmann F, Labbé P, Justy F, Weill M, Sicard M. The cellular phenotype of cytoplasmic incompatibility in Culex pipiens in the light of cidB diversity. McGraw EA, editor. PLoS Pathog. 2018; 14:e1007364. https://doi.org/10.1371/journal.ppat.1007364 PMID: 30321239
- 109. Brandriff B, Pedersen RA. Repair of the ultraviolet-irradiated male genome in fertilized mouse eggs. Science. 1979; 1981(212):1431–1433. https://doi.org/10.1126/science.7466400 PMID: 7466400
- Shropshire JD, Rosenberg R, Bordenstein SR. The impacts of cytoplasmic incompatibility factor (cifA and cifB) genetic variation on phenotypes. Genetics. 2021. https://doi.org/10.1093/genetics/iyaa007
 PMID: 33683351
- Beckmann JF, Ronau JA, Hochstrasser M. A Wolbachia deubiquitylating enzyme induces cytoplasmic incompatibility. Nat Microbiol. 2017: 2. https://doi.org/10.1038/nmicrobiol.2017.7 PMID: 28248294
- 112. Sun G, Zhang M, Chen H, Hochstrasser M. The CinB Nuclease from w No Wolbachia Is Sufficient for Induction of Cytoplasmic Incompatibility in Drosophila. MBio. 2022: 13. https://doi.org/10.1128/mbio.03177-21 PMID: 35073749
- 113. Cooper BS, Ginsberg PS, Turelli M, Matute DR. Wolbachia in the Drosophila yakuba complex: Pervasive frequency variation and weak cytoplasmic incompatibility, but no apparent effect on reproductive isolation. Genetics. 2017; 205:333–351. https://doi.org/10.1534/genetics.116.196238 PMID: 27821433
- 114. Poinsot D, Bourtzis K, Markakis G, Savakis C, Merçot H. Wolbachia transfer from Drosophila melanogaster into D. simulans: Host effect and cytoplasmic incompatibility relationships. Genetics. 1998. https://doi.org/10.1093/genetics/150.1.227 PMID: 9725842
- 115. Zabalou S, Apostolaki A, Pattas S, Veneti Z, Paraskevopoulos C, Livadaras I, et al. Multiple rescue factors within a Wolbachia strain. Genetics. 2008; 178:2145–2160. https://doi.org/10.1534/genetics. 107.086488 PMID: 18430940
- 116. Kaur R, Martinez J, Rota-Stabelli O, Jiggins FM, Miller WJ. Age, tissue, genotype and virus infection regulate Wolbachia levels in Drosophila. Mol Ecol. 2020; 29:2063–2079. https://doi.org/10.1111/mec. 15462 PMID: 32391935
- 117. Clemons A, Haugen M, Flannery E, Tomchaney M, Kast K, Jacowski C, et al. Aedes aegypti: An emerging model for vector mosquito development. Cold Spring Harb Protoc. 2010; 5. https://doi.org/10.1101/pdb.emo141 PMID: 20889691
- 118. Juhn J, James AA. Hybridization in situ of salivary glands, ovaries, and embryos of vector mosquitoes. J Vis Exp. 2012:1–18. https://doi.org/10.3791/3709 PMID: 22781778
- 119. Page J, Berríos S, Rufas JS, Parra MT, Suja JÁ, Heyting C, et al. The pairing of X and Y chromosomes during meiotic prophase in the marsupial species Thylamys elegans is maintained by a dense plate developed from their axial elements. J Cell Sci. 2003; 116:551–560. https://doi.org/10.1242/jcs.00252 PMID: 12508115
- 120. Viera A, Parra MT, Arévalo S, de la Vega CG, Santos JL, Page J. X chromosome inactivation during grasshopper spermatogenesis. Genes (Basel). 2021: 12. https://doi.org/10.3390/genes12121844 PMID: 34946793